CCS Chemistry

MINI REVIEW

Received: Jan. 15, 2024 | Accepted: Feb. 23, 2024 | Published: Mar. 12, 2024

Metal–Organic Frameworks Housing Active Molecules as Bioinspired Catalysts

Yin Zhang[1], Peter E. VanNatta[1], Junyu Ren[2] & Shengqian Ma[1]*

[1]*Department of Chemistry, University of North Texas, Denton, Texas 76201,* [2]*Department of Chemical and Biomolecular Engineering, National University of Singapore, Singapore 117585*

**Corresponding author: shengqian.ma@unt.edu*

Cite this: *CCS Chem*. **2024**, 6, 1380–1402
DOI: 10.31635/ccschem.024.202403909

Optimization of activity, selectivity, and stability of catalysts for practical application is a long-sought-after goal. Recent progress in the advancement of rational catalyst design routinely takes queues from nature. Specifically, enzymes are renowned for their high efficiency and selectivity in diverse and significant reactions under mild conditions. Despite the well-known merits of enzymes, they often remain unsuitable for industrial catalysis due to issues, including limited environment (solvent/temperature/pH) compatibility, considerable structural uncertainty, and highly specific reaction scopes. In the context of bioinspired catalysis design, the development of synthetic heterogeneous catalyst analogs, which may not only mimic enzymes to reproduce or even surpass their performance but also bypass their intrinsic limitations, is thus, desirable and has been extensively studied in the context of porous materials. The metal–organic framework (MOF) is a superior candidate for porous materials towards this goal, thanks to facile and modular preparation, explicit crystalline composition/structure, tunable pore size/environment, and excellent stability. The introduction of active molecular species such as bioactive molecules (e.g., proteins, enzymes, peptides, amino acids, porphyrins) and chemically active molecules (e.g., frustrated Lewis pairs) into metal–organic frameworks (MOFs) via pore encapsulation, chemical postmodification, or bottom-up construction has been shown to facilitate the cooperative enhancement of catalysis through the enforcement of proximity, enhancement of control/activity, and even inducement of unexpected selectivity. In this minireview, we sought to summarize the last 5 years of fruitful progress, exploiting MOFs housing active molecules for substantial catalysis applications, including asymmetric reactions, CO_2 conversion (reduction, cycloaddition), biocatalytic H_2O_2/dye degradation, and so on, and discuss challenges and opportunities in the prospective exploration of these systems towards enzyme mimicry and new-to-nature catalysis.

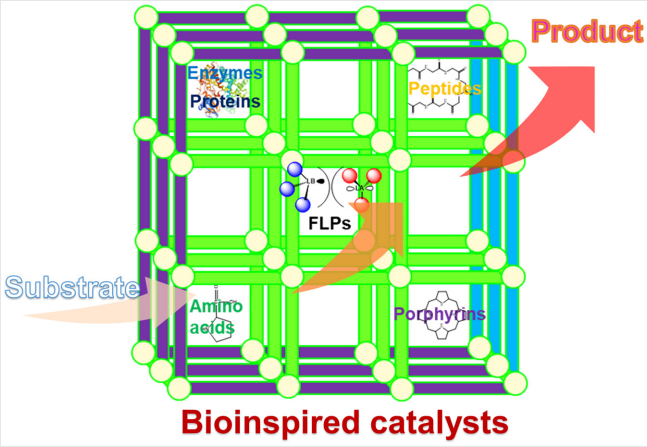

Keywords: metal–organic framework, bioinspired catalyst, active molecular species

Introduction

The development of practical catalysts for highly efficient and task-specific transformations under mild conditions is a principal goal of catalysis research.[1] Nature provides a tremendous reservoir of systems catalyzing critical transformations such as CO_2 fixation, water oxidation, and hydrogenation under ambient conditions. These significant transformations are intrinsically accomplished by a vast number of active macromolecular species (mainly enzymes), which are continually being characterized and reported as composed of versatile multimeric assemblies.[2] Efforts to understand the high efficiency and selectivity of these active catalysts have laid the solid foundation of the modern chemical/biochemical industry. Nonetheless, natural limitations, including narrow effective temperature range, vulnerability to the reaction environment, and requirement of high-accuracy substrate-active site orientation have largely hampered their practical usage.[3-9] In this background, synthetic catalysts have been in intense demand.

Occurring as a prevalent theme, molecular catalysts with bioinspired active sites are continually being pursued, though the selectivity and reusability of catalysts remain a significant challenge.[10] As a promising answer to this challenge, supramolecular catalysts have emerged as a higher fidelity paradigm, resembling enzymes to a closer extent with active sites protected within the cavity.[11] Unfortunately, their relatively low flexibility and stability, moreover, structural uncertainty, hinders mechanistic elucidation, achieving optimization. As a higher stability alternative, porous polymers have proven superior; however, their irregular pores and intractable crystallinity similarly limit mechanistic elucidation. Given the stated shortcomings of the aforementioned catalyst classes, catalysts built on porous crystalline materials such as metal–organic frameworks (MOFs) appear to merge the strengths of both while eliminating the undesirable characteristics (Figure 1a,b). Indeed, the recent progress observed over the last 5 years cements this motif as best able to achieve enzymatic effectiveness as well as facilitate elucidation of structure-property correlations.

For the purpose of this minireview, we limit our discussion to MOFs as the prototypical porous crystalline material for housing active molecules as biomimetic catalysts. To achieve enzymatic effectiveness, catalysts with enzyme-mimicry of three types can be pursued: (1) structural mimicry; (2) compositional mimicry; (3) simultaneous structural and compositional mimicry.

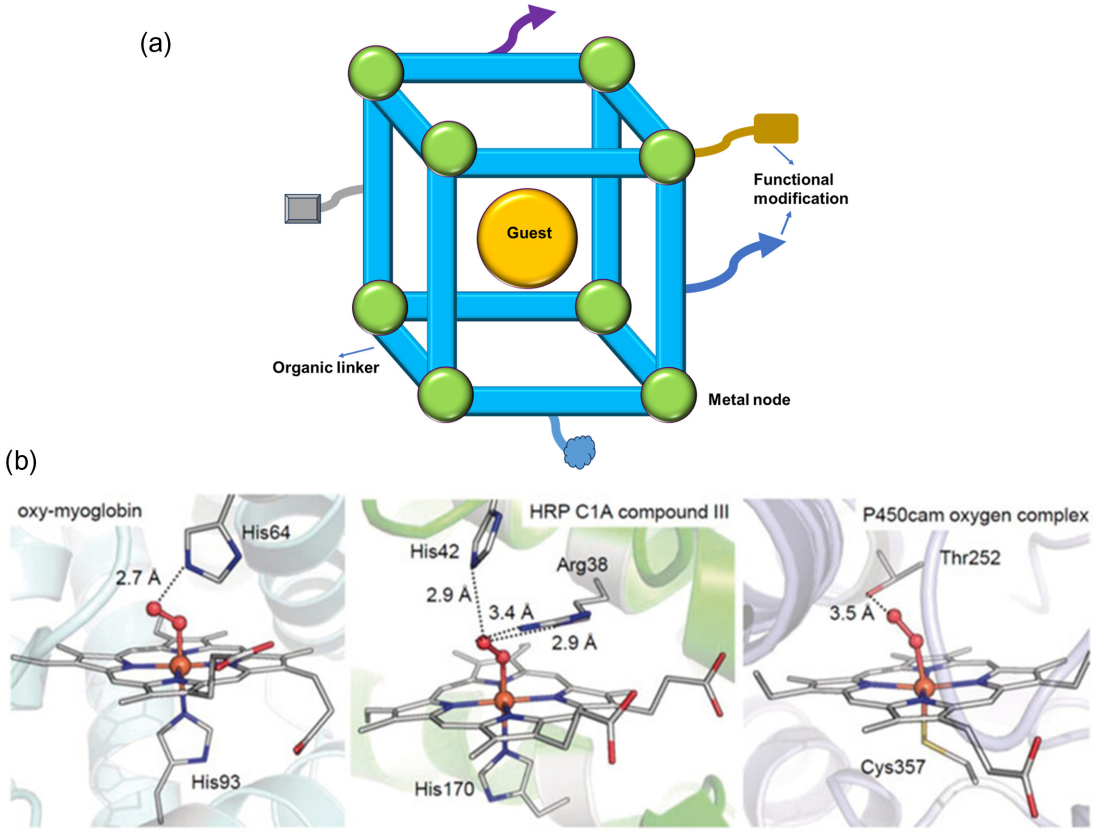

Figure 1 | *MOF catalysts (a) versus enzymes (b). Panel (b) reproduced with permission from ref 121. Copyright 2020 John Wiley & Sons, Inc. MOFs featuring robust structure, modifiable versatility, and controllable porosity are indispensable merits for the construction of bioinspired catalysts in close proximity. MOF, metal–organic framework.*

DOI: 10.31635/ccschem.024.202403909
Citation: *CCS Chem.* **2024**, 6, 1380–1402
Link to VoR: https://doi.org/10.31635/ccschem.024.202403909

We have focused mainly on the structural mimicry of enzymes by MOF catalysts with in-pore active sites, which, in some cases, are modified with functional sites in the vicinity for establishing second-sphere interactions.

MOFs are a type of crystalline hybrid materials constructed from the dative linkage of metal ion/metal oxide cluster nodes and organic linkers spanning variable morphological dimensions, structures, and compositions.[12] In this way, MOFs not only resemble homogenous molecular catalysts with high flexibility, tunability, and abundant reactivity but also have the intrinsic advantages of heterogeneous catalysts; namely, superior separability, recyclability, and stability. In general, the attraction and activation of substrate by MOFs can be expected to be efficient owing to their high surface energy. Of particular importance, MOFs typically possess periodic porosity with expansive pore sizes from micropores to mesopores and have tunable pore environments. This allows MOF-based catalysts to overcome the mass-transfer issues that are usually endemic in irregular porosity polymers and zeolites of small pore sizes and affords the additional benefit of specific and tunable size-selective control over substrate access. Furthermore, the confinement effect induced by the periodic and ordered pore structure and the second-sphere interactions enabled by the rational design of the pore environment can further boost the reaction efficiency and selectivity. Based on the merits endowed by their morphologies and structures, MOFs have been deemed a next-generation of heterogeneous catalysts.

MOFs are well known to facilitate catalysis through flexible compositional manipulation. This has been achieved by fully taking advantage of their modular nature to intentionally introduce functionality on metal nodes and/or organic ligands during/post MOF preparation, rendering MOFs capable of task-specific catalysis. For example, given the variety of reactivity and superior activity of molecular metal complexes in organic/organometallic chemistry, particularly noble metal-based complexes, the incorporation of active metal centers in MOF structures has been extensively studied for crucial transformations, including hydrogenation, C–H activation, and even methane oxidation. Of note, all these metals are a nonrenewable and limited resource, even though the immobilized active metal sites on MOFs are recyclable, in contrast with their homogenous enzyme-mimicking counterparts. To overcome this constraint, and more importantly, to enable artificial enzymatic conversion under mild conditions, active molecular species, including regenerable bioactive molecules and underdeveloped nonmetal-based chemically reactive entities have been introduced into MOFs and have generated immense interest.[13] Naturally abundant and variable bioactive molecules such as amino acids, peptides, proteins, and enzymes have thus, largely expanded the composite library. Meanwhile, frustrated Lewis pairs (FLPs), a bifunctional combination of a bulky Lewis acid and a bulky Lewis base, have emerged as a type of striking catalyst, with the potential to realize challenging activation of small molecules and C–H bonds under ambient conditions.[14–17] Furthermore, the majority of reported molecular FLPs are composed of naturally abundant nonmetal/main group elements, a valuable consideration for deployment at scale, and have realized facile incorporation into MOFs, resulting in enzymatic-like catalytic enhancement in addition to the advantages intrinsic to heterogeneous materials.[18] It has been demonstrated that, after the introduction of catalytically active molecular species into MOF hosts, the composite could retain the guests' activity, and enhance their thermal stability, solvent tolerance, as well as shelf-life. In addition, this paradigm enables the creation of versatile catalysts without the uncertainty of assembling different functional parts as is prevalent in multimeric enzymes. Apart from the performance of the active molecular species themselves, the fusion with MOFs gives rise to a synergistic effect, exhibiting novel performance beyond the constituents, thereby turning this kind of combination into a cooperative catalyst. As a result, a multitude of catalysts have been facilely prepared and diverse transformations with a broader scope than the individual active molecular entities have been realized. Exclusively, these catalysts exhibit outstanding activity and selectivity due to host-induced synergistic effects, confinement effects, and size selectivity. MOFs with active molecular species have, therefore, become a prevalent class of catalysts, attracting tremendous interest from researchers in the fields of functional materials, catalysis, medicinal chemistry, biochemistry, and more.

This minireview presents the pioneering and continuing progress (primarily over the last 5 years) in the design and preparation of MOFs with active molecular species for catalysis. We highlight pore encapsulation, chemical postmodification, and bottom-up construction as easy and operational methods that combine the individual functionality of host and guest, resulting in the rational design and modular synthesis of diverse and versatile catalysts. Their crucial applications have also been summarized considering the new host–guest catalysts' applicability for industrially significant yet challenging reactions, including the new-generation asymmetric catalysis. Ongoing work and prospects in this direction are discussed, with the hope of further inspiring researchers worldwide towards the advancement of these materials for practical applications in catalysis and beyond.

The Construction of Desirable Catalysts of MOFs Housing Active Molecular Species

Sustainable catalysis has become a forefront topic and has fueled the development of novel heterogeneous

DOI: 10.31635/ccschem.024.202403909
Citation: *CCS Chem.* **2024**, 6, 1380–1402
Link to VoR: https://doi.org/10.31635/ccschem.024.202403909

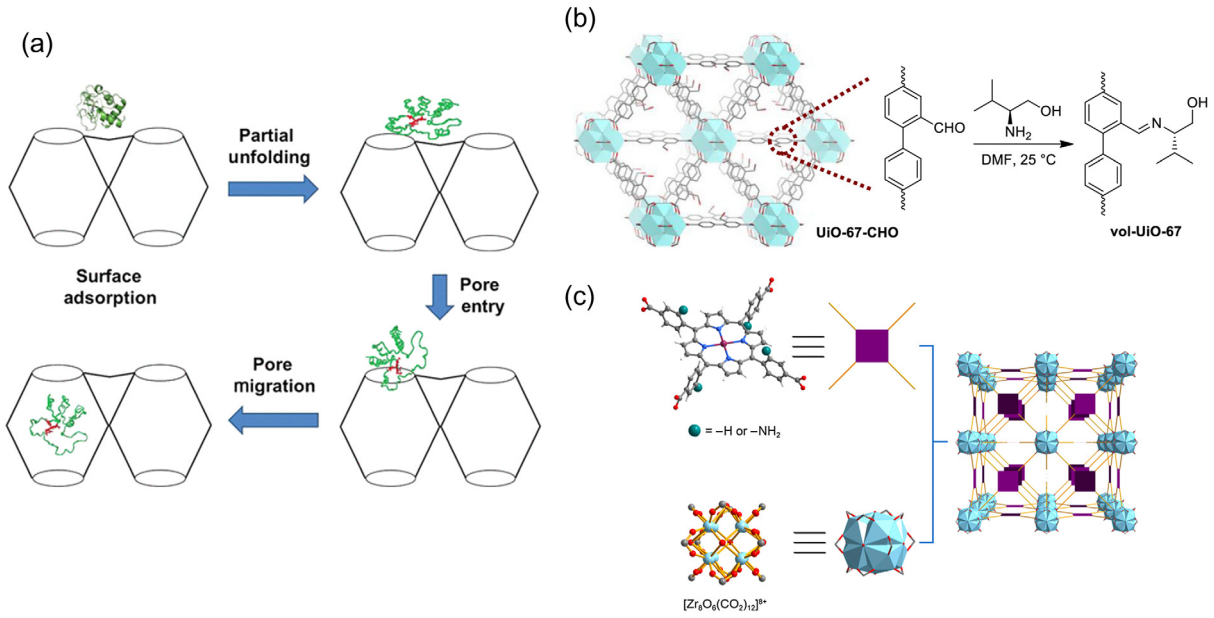

Figure 2 | *The strategy for constructing catalysts of MOF housing active molecular species. (a) Pore encapsulation. Reproduced with permission from ref 21. Copyright 2012 ACS Publications. (b) Chemical postmodification. Reproduced with permission from ref 36. Copyright 2021 ACS Publications. (c) Bottom-up construction. Reproduced with permission from ref 98. Copyright 2023 CCS Publications. MOF, metal–organic framework.*

catalysts. Nature has created renewable enzymes of assembled functional entities for myriad transformations. Crystallographic determination of enzymes and corresponding mechanistic investigation by virtue of comprehensive contemporary techniques has shown the essential role inside-cavity active sites and second-sphere interactions play in achieving exceptional activity and selectivity under biological conditions. In pursuit of artificial catalysts with comparable, or even better performance as enzymes, as well as enhanced reaction environment compatibility, MOFs housing catalytically active molecular species, including regenerable bioactive molecules and underdeveloped chemically reactive entities have emerged as an excellent prototype. The flexibility of reticular chemistry facilitates the modular construction of target catalysts; in total, three efficient methods have been adopted to complete this task: pore encapsulation, chemical postmodification, and bottom-up construction (Figure 2a–c).

Pore encapsulation

Starting from their emergence, pore engineering of MOFs has been a crucial subject, accounting for the creation of permanent micropores (<2 nm), mesopores (2–50 nm), and even macropores (>50 nm) within their structures.[19] Beyond the exciting performance using pristine MOFs for catalysis, gas storage/separation, and water remediation, the promising capacity for complex materials associated with the incorporation of guest species as a pore-size/environment modification and functional mediator, provides the opportunity for the development of novel catalysts to produce chemical commodities to meet increasing global demand. As such, physical interactions, including Van der Waals interaction and electrostatic interaction, have been exploited to rationalize and accelerate the introduction of active small molecules and macromolecules into MOF pores.

Our group first reported the successful immobilization of microperoxidase-11 (MP-11) into mesoporous Tb-mesoMOF in 2011.[20] Specifically, freshly synthesized Tb-mesoMOF crystals, which possess hierarchical cavities of 3.9 and 4.7 nm diameter, were immersed in MP-11 (dimensions of about 3.3 × 1.7 × 1.1 nm) solution of 4-(2-hydroxyethyl)-1-piperazineethanesulfonic acid (HEPES) buffer, and placed in an incubator at 37 °C. To validate the successful incorporation of MP-11 and reveal the corresponding mechanism, surface area measurement, and single-crystal optical absorption spectroscopy were conducted. N_2 sorption isotherms measured at 77 K showed that the Brunauer–Emmett–Teller (BET) surface area of Tb-mesoMOF decreased from 1935 to 400 m^2/g after saturation with MP-11. Pore size distribution analysis found that the pore size of the resultant sample was mainly around 0.9 nm, accompanied by the disappearance of primitive mesopores. These results indicated the successful encapsulation of MP-11 into Tb-mesoMOF. Meanwhile, it turned out that the absorption spectrum of MP-11@Tb-mesoMOF exhibited a Soret band at ~410 nm, while the corresponding Soret band of MP-11

DOI: 10.31635/ccschem.024.202403909
Citation: *CCS Chem.* **2024**, 6, 1380–1402
Link to VoR: https://doi.org/10.31635/ccschem.024.202403909

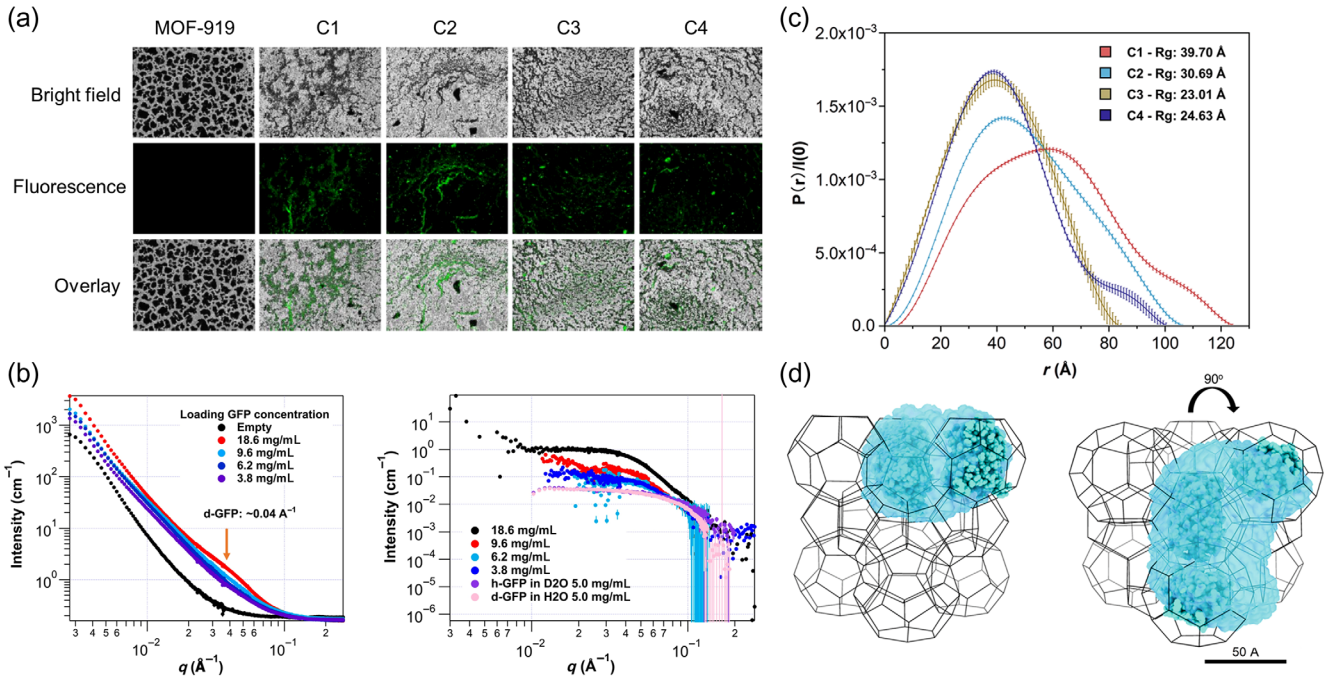

Figure 3 | *Featured characterization of d-GFP@MOF-919 catalysts. (a) Fluorescent microscopy images of MOF-919 before and after the inclusion of d-GFP (C1–C4) under bright field, fluorescence, and overlay. (b) SANS profiles of d-GFP@MOF-919 (C1–C4) before (left) and after (right) the subtraction of MOF scattering at the contrast matching point 50% D_2O. (c) Experimental P(r) curves for d-GFP loaded in the MOF-919 (C1–C4). (d). Ab initio structure reconstruction of C2 in the structure of MOF-919. Reproduced with permission from ref 23. Copyright 2023 Springer Nature Limited. GFP, green fluorescent protein; MOF, metal–organic framework; SANS, small-angle neutron scattering.*

in buffer solution was 400 nm. Thus, the interactions between the trapped MP-11 molecules and the hydrophobic nanoscopic cages were revealed by means of a bathochromic shift of the encapsulated MP-11 in the Tb-mesoMOF. This work opened a new avenue for encapsulating enzymes in MOFs for applications like heterogenous biocatalysis and beyond. Moreover, this research inspired numerous studies aimed at understanding the interactions between MOFs and active biomolecules, as well as their conformations inside MOFs, which, in turn, has served to bolster the design of advanced composite materials and disclose the correlation between structure and performance. To follow up, we intended to ascertain the specific interactions stabilizing MP-11,[21,22] which might intrinsically distinguish MOFs from the widely used amorphous porous materials such as mesoporous silica. Therefore, Raman spectroscopy was performed on MP-11@Tb-mesoMOF, MP-11, and Tb-mesoMOF in the HEPES buffer. The results suggested the existence of strong π···π interactions between the heme and conjugated triazine and phenyl rings of the 4,4′,4″-*s*-triazine-2,4,6-triyltribenzoate (TAPB) ligand in MP-11@Tb-mesoMOF. Compelling evidence of this interaction came from two peaks observed at 1317 and 1567 cm^{-1}, assigned to the C–H bending and C=C stretching modes of the heme, respectively, which exhibited a redshift compared with MP-11. Correspondingly, characteristic vibrational peaks of 2,4,6-triamino-1,3,5-trinitrobenzene (TATB) in MP-11@Tb-mesoMOF underwent obvious shifts in contrast to Tb-mesoMOF, displaying signals at 990, 1054, 1409, and 1610 cm^{-1}. Thus, the interactions between the encapsulated enzyme guest and MOF host were clearly unveiled.

To further query the spatial arrangement of active biomolecules infiltrated in MOFs, we used the in situ small-angle neutron scattering (SANS) technique (Figure 3a–d).[23] Unlike conventional spectroscopic analysis such as Fourier-transform infrared (FT-IR) spectroscopy, solid-state UV–visible spectrophotometry, and Raman spectroscopy provide indirect evidence. SANS enabled high-resolution spatial mapping of guest molecules, including biomolecules, within the porous matrix. This was predicated on twofold preconditions: (1) SANS has a resolution at length scales of ~1 to 200 nm that covers the diameter of catalytically bioactive molecules; (2) it can minimize scattering interference from the matrix by tuning scattering contrast of solvent with the variation of deuterated and hydrogenated solvents. As proof of concept, green fluorescent protein (GFP) was chosen as a model entity and measured before and after combination with water-stable MOF-919 via pore encapsulation. We started with the survey on matrix MOF-919.

DOI: 10.31635/ccschem.024.202403909
Citation: *CCS Chem.* **2024**, 6, 1380–1402
Link to VoR: https://doi.org/10.31635/ccschem.024.202403909

The hierarchical structures of MOF were reflected by three regions accounting for its inhomogeneity and ordered pore arrangement in the q-range of 0.0015 < q < 0.5 Å^{-1}. As neutron contrast depends on the isotopic composition of scattering objects and surrounding media, a hydrogenated/deuterated water mixture was introduced to saturate the MOF, aimed to identify the ideal contrast matching point crucial to suppress the matrix contrast from the composites and subsequently, highlight the guest molecules. A 50% D_2O volume ratio of the mixture solvent was determined as an optimal point. The SANS profile of MOF-919 in this mixture solvent witnessed the disappearance of the signal at the high q peaks and a considerable increase of background compared with a dry sample and was attributed to the penetration of water molecules into the accessible pores and the incoherent scattering of H_2O in the mixture solvent, respectively. Switching to the study on GFP@MOF-919, deuterated-GFP (d-GFP) rather than hydrogenated-GFP (h-GFP) was adopted to increase its contrast to matrix MOF. SANS measurement on d-GFP@MOF-919 samples with different loading amounts of d-GFP revealed that the scattering intensity exhibited a drastic increase in the whole q range compared with that of empty MOF in 50% D_2O. Particularly, along with increasing the loading amounts of d-GFP, a broad shoulder ascends in the mid q region near ~0.04 Å^{-1}, diagnostic of the hosted d-GFP. Collectively, these results confirmed the successful encapsulation of d-GFP. Further analysis and three-dimension reconstruction have shown that each d-GFP monomer was not denatured but maintained its native conformation, and tended to arrange closely and assembled multimers inside the mesopores of MOF-919, particularly, at high loading amounts due to the existence of protein-protein interactions and the confinement effect. In this way, we have developed a novel and noninvasive approach to probe the behaviors of biomolecules in the nanospaces of MOFs by taking advantage of sophisticated techniques; this will be of importance for applications, including catalysis.

Pore encapsulation has also been extensively expanded by other groups to prepare composite catalysts. Among them, Farha's group[5] has contributed significantly with several intriguing works using judiciously designed high-stability zirconium-based mesoporous MOFs and variable biomolecules with different functionalities. Particularly, NU-1000, consisting of 8-connected Zr_6 nodes and 4-connected linkers of 1,3,6,8-tetrakis(p-benzoic-acid)pyrene (H_4TBAPy) ligand, was utilized as a superior support for accommodating guest molecules because of its formation of hierarchical triangular and hexagonal mesoporous structures with the size of ~30 Å and micropores with the size of ~12 Å.[5] In representative work, NU-1000 was selected to accommodate an esterase cutinase (3 × 3 × 4.5 nm) because of its appropriate porosity and resistance to reaction conditions.[24] To quantify the uptake of cutinase by NU-1000-5 μm, UV–visible spectroscopy and inductively coupled plasma-optical emission spectroscopy (ICP-OES) were utilized together giving a maximum uptake of 5 μmol/g. Furthermore, in situ confocal laser scanning microscopy (CLSM) was employed to elucidate the dynamics of enzyme loading into the pores of NU-1000. Deploying an Alexa-Fluor 647-labeled enzyme (Cut647), it was demonstrated that the dye-labeled enzyme entered the MOF and was directed to the center of NU-1000 as a function of immersion time. Additionally, the size of NU-1000 particles was found to indeed affect the enzyme encapsulation process, affording a 10-fold increase in efficiency by decreasing the size from 10 to 1.5 μm. The interaction between cutinase and NU-1000 has also been discussed and is attributed to columbic forces, as isoelectric point determinations gave values of approximately pH 7.8 and pH 4.3 for cutinase and NU-1000, respectively, corresponding to the generation of positive and negative charged species in a pH 7 buffer solution. NU-1000 has also been successfully employed to encapsulate and stabilize the protein, insulin (1.3 × 1.3 × 3.2 nm) because of the electrostatic and/or hydrophobic interactions between insulin and the MOF surface.[25] Successively, a catalytically active enzyme cytochrome c (Cyt c, 3.2 × 2.7 × 3.8 nm) has also been introduced into the nanospace of NU-1000.[26] In another work, the pore environment of NU-1000 was pre-ornamented by the amino acids L-serine and betaine to investigate how the chemical environment of pores affect the subsequent encapsulation of the protein ubiquitin (1.9 × 1.9 × 2.4).[27] Farha's group[28] also reported the application MOF consisting of porous coordination network yellow material (PCN-128y), with a mesoporous channel of 4.4 nm to shield organophosphorus acid anhydrolase (OPAA; 4.4 × 4.4 × 7.8 nm), which is a nerve agent detoxifying enzyme. Very recently, they devised a semi-artificial photocatalytic system by incorporating formate dehydrogenase (FDH; 6 × 4 × 11 nm) into light-harvesting scaffold NU-1006 which was pre-anchored by an electron-mediator Rhodium (Rh) complex (Cp*Rh(bpydc)Cl, bpydc = 2,2′-bipyridyl-5,5′-dicarboxylic acid).[29] This collection of impressive work has largely expanded and diversified the field of using MOFs as a tunable platform for protecting enzymes and other proteins from denaturation via pore encapsulation.

Similarly, the enzyme esterase *Alicyclobacillus acidocaldarius* EST2 (AaEST2) has been incorporated into the pores of NU-1000 by simply immersing NU-1000 powder into Tris-buffered solutions containing a specific amount of esterase AaEST2.[30] Apart from the utilization of aforementioned NU-series MOFs as porous supports for encapsulation, PCN-333(Al),[31] The chromium terephthalate MOF (MIL-101 series; MIL = Matérial Institut Lavoisier),[32] and a zirconium family of MOF (UIO-67; UIO = University of Oslo)[33] have also been successfully implemented as

DOI: 10.31635/ccschem.024.202403909
Citation: *CCS Chem.* **2024**, 6, 1380–1402
Link to VoR: https://doi.org/10.31635/ccschem.024.202403909

enzyme encapsulation supports by different research groups. It should be emphasized that all these examples confirm how the diameter match between MOF pore and guest species plays a crucial role in successful pore encapsulation. In addition, possible interactions between host and guest should also be adequately considered, as these play a pivotal role in guest loading. Complementary characterizations based on advanced instruments and techniques have been comprehensively established for verifying the successful encapsulation, quantifying the uptake amount, disclosing mutual interactions, and visualizing the spatial arrangement of encapsulated catalytically active molecules. These techniques are valuable for rational catalyst design toward optimized performance.

Chemical postmodification

Another important strategy for combining active moieties with MOFs involves the utilization of chemical bonding/interactions to anchor the two components. The rich foundation established to date regarding the postmodification of MOFs facilitates both MOF design and methodology and fosters the evolution of a new category of catalysts using MOF hosts with active guest molecules. With the guest moiety and substrate scope in mind, one can readily search the MOF library for candidates with appropriate pore structure, surface area, open metal sites, and intrinsic/built-in functional groups. In the case of a failure to find a MOF within the thousands reported to meet specific requirements, novel design, and synthesis of functional MOFs can also leverage the numerous studies covering ligand synthesis and crystallographic principles.

Amino acids are the smallest building blocks of peptides and proteins; therefore, they are intrinsically linked to biocatalysis serving as the source of chiral catalyst/auxiliary agents, thereby enabling selectivity of asymmetric catalysis in nature. Due to their small sizes, they are efficiently manipulated for postmodification of porous MOFs. For example, in 2021, the Tanase group[34] reported the construction of chiral catalysts through the coordination of chiral proline onto the open metal site of MOF-74(Zn) which has a channel ca. 1.5 nm larger than the size of proline. The amino acid coordinates to Zn sites in a monodentate manner via its carboxylate group and the coordination strength in *N,N′*-dimethylformamide (DMF) is much stronger than in methanol, leading to a better performance of chirality introduction. The strong coordination of the chiral proline in DMF on Zn sites resulted in controlled defect generation and pore blocking, likely to become powerful mediators of future catalytic systems. Aside from postmodification at the metal nodes of MOFs, the introduction of chiral amino acids at organic linkers has also been reported. In 2021, the Manna group[35] provided a general method for the preparation of MOF-based single-site chiral catalysts with naturally occurring amino acids and earth-abundant base metals. As a prime example, UIO-68-NH_2 was selected as the platform to graft chiral amino acids, including L-valine, L-alanine, and L-leucine via amide coupling between the amino-group of the MOF and the carboxylic acid group of N-9-fluorenylmethyloxycarbonyl (N-Fmoc)-protected amino acid. This process resulted in the introduction of strong chiral induction and plentiful coordination sites within the pores of UIO-68-NH_2. To further facilitate the coordination of active molecules, deprotection of the amino group and treatment with picolinaldehyde yielded the corresponding chiral tridentate nitrogen-donor amino acid-pyridylimine ligand functionalized MOFs: L-valim-UiO, L-alaim-UiO, and L-leucim-UiO. From these scaffolds, iron-based enantioselective hydrosilylation catalysts were obtained via amide deprotonation by *sec*-butyllithium (*sec*-BuLi) and subsequent metalation with $FeCl_2$; the final forms defined as L-valim-UiO-FeCl, L-alaim-UiO-FeCl, and L-leucim-UiO-FeCl, respectively. The maintained crystallinity during lithiation and metalation, base-metal loadings, and porosity were readily confirmed by powder X-ray diffraction (PXRD), ICP, and N_2 sorption measurements, respectively. To gain insight into the amino acid-endowed chiral and coordination environments around Fe sites, complementary supports from both experiments and computations have been presented. X-ray absorption near edge structure (XANES) and extended X-ray absorption fine structure (EXAFS) analyses of L-valim-UiO-FeCl indicated that each iron center was divalent and coordinated with three nitrogen atoms of the chelating valim-ligand, along with one chloride and one oxygen atom from tetrahydrofuran (THF). Meanwhile, the density functional theory (DFT)-optimized structure was consistent with the EXAFS fitting results, revealing a five-coordinate iron species of L-valim-FeCl(THF) within the MOF as the ground state. Within a short time, the same group made another contribution, offering a simplified strategy by using the chiral amino alcohol (valinol) instead to functionalize the aldehyde-containing UiO-68 (67)-CHO via a condensation reaction between the amino-group of valinol and the aldehyde group of UiO-68 (67)-CHO, obtaining the final chiral catalyst, following $FeCl_2$ coordination.[36] These two reports have spurred the development of atom- and source-economy catalysts desirable for practical transformations.

Inspired by nature and building upon the seminal work describing the incorporation of amino acids in MOFs, the aim to develop catalysts with multiple interactive sites and enhanced chiral environments has inspired the expansion toward the incorporation of small peptides in MOFs. The Mellot-Draznieks group[X] has recently reported the generation of a chiral heterogeneous catalyst through the introduction of a chiral peptide into a MOF in cooperation with active metal sites.[37] In this study, the catalyst was prepared from a chemical

DOI: 10.31635/ccschem.024.202403909
Citation: *CCS Chem.* **2024**, 6, 1380–1402
Link to VoR: https://doi.org/10.31635/ccschem.024.202403909

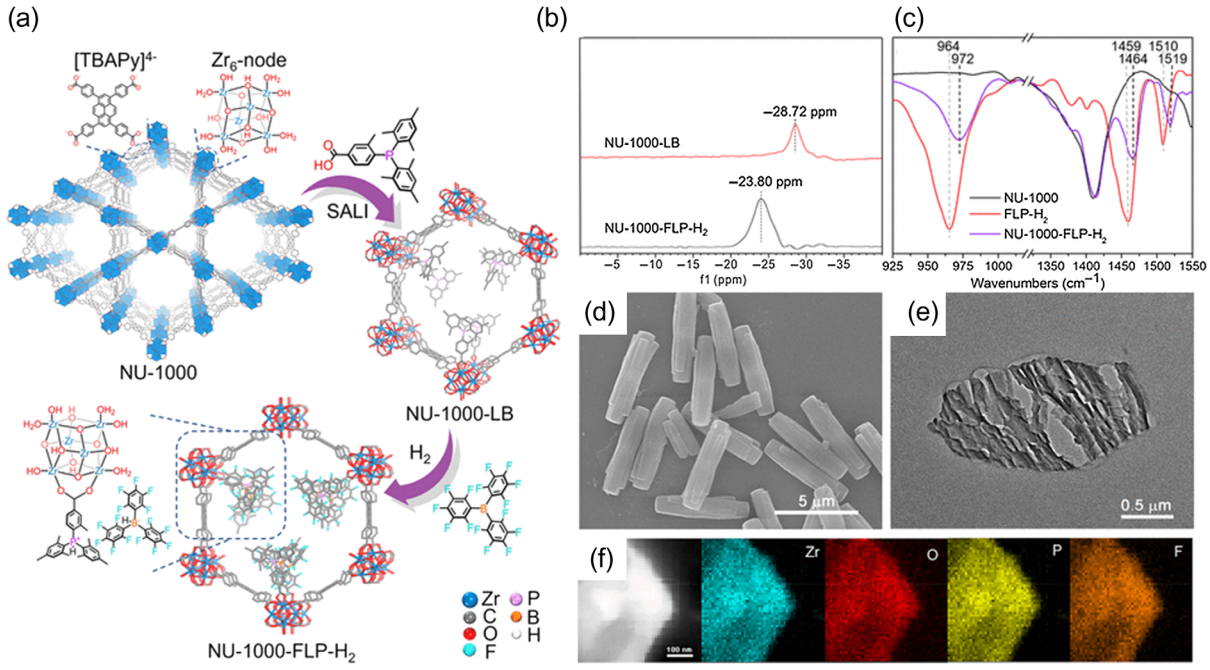

Figure 4 | *The preparation and characterization of P/B FLP@NU-1000 catalysts. (a) The construction of P/B FLP@NU-1000 via a stepwise anchoring strategy. (b) Solid ^{31}P Magic Angle Spinning NMR spectra of Nu-1000-LB (LB: Lewis base) and Nu-1000-FLP-H_2 indicate the successful introduction of Lewis base and active P/B FLP-H_2 to NU-1000. (c) FT-IR spectra of Nu-1000, FLP-H_2, and Nu-1000-FLP-H_2 display characteristic peaks that suggest the successful anchoring of FLP-H_2 in MOF. (d–f) Transmission electronic microscopy and elemental mapping images of Nu-1000-FLP-H_2. Reproduced with permission from ref 56. Copyright 2023 ACS Publications. FLP, frustrated Lewis pairs; NMR, nuclear magnetic resonance; MOF, metal–organic framework.*

modification of Al-MIL-101-NH_2 with the peptide L-GlyProBoc (Gly: glycine, Pro: proline) via an amidation reaction, followed by metalation with an in situ generated $[(C_6H_6)Ru(acn)_3][NO_3]_2$ (acn = acetonitrile) agent from a commercially available dimeric (arene) Ru complex. The Ru monomer coordinates with two nitrogen atoms of the peptide-functionalized MOF to yield the active catalyst. Interestingly, it was found that the metalation failed when a single amino acid of proline was modified on the wall of MIL-101-NH_2. This finding was attributed to steric hindrance between the MOF walls and the complex; whereas the Gly component provided an essential spacer to the coordinating amino acid.

The variety and diversity of modern synthetic chemistry empower many options to vary reactivity and selectivity aside from peptides. FLP adds another dimension to fulfill this option and has raised extensive interest across multiple fields of the scientific community.[14–17] The definition of FLP describes the expected yet lack of bonding between bulky Lewis acids and Lewis bases as a result of steric hindrance, leading to the formation of an interactive pair, which are found to be highly active, exhibiting notable capability in activation of small molecules (H_2, CO_2, etc.), C–F bonds, and C–H bond under mild conditions. The rapid progress made in homogeneous FLP catalysis has also inspired the advancement in heterogenous catalysis targeting reusable catalysts with improved performance and reaction environment compatibility.[18,38–59] Our group has demonstrated the first example of constructing heterogeneous FLP catalysts based on porous materials, including MOFs.[38] In a recent report, we judiciously employed a stepwise anchoring strategy to introduce a classic FLP composed of 1,4-diazabicyclo[2.2.2]octane (DABCO) as the Lewis base and tris(pentafluorophenyl)borane (BCF) as the Lewis acid into the nanospace of MIL-101(Cr). One nitrogen atom of bifunctional DABCO anchoring on open Cr^{III} metal sites of the secondary building unit (SBU) $Cr_3(\mu_3\text{-}O)(COO)_6(OH)$ of the dehydrated MOF MIL-101 (Cr) established the crucial connection between MIL-101(Cr) and Lewis base. Subsequent addition of BCF generated the target FLP@MIL-101(Cr) catalyst. PXRD patterns and electron microscopy images revealed that FLP@MIL-101 (Cr) maintained the crystallinity and morphology of parent MIL-101(Cr). The successful introduction of FLP into MOFs was confirmed by complementary results obtained from comprehensive measurements. Firstly, the compositional combination of two parts was supported by FT-IR, X-ray photoelectron spectroscopy (XPS), and energy dispersive X-ray spectroscopy (EDS) elemental

DOI: 10.31635/ccschem.024.202403909
Citation: *CCS Chem.* **2024**, 6, 1380–1402
Link to VoR: https://doi.org/10.31635/ccschem.024.202403909

mapping, showcasing the characteristic signal of each component of the FLP. Moreover, analysis of the XPS spectra revealed a 1 eV shift of the Cr 2p signal toward higher binding energy, verifying the interaction between the Cr metal sites and the Lewis base. N_2 sorption test results showed an evident decrease in BET surface area (from 2724 to 1013 m^2/g) and a reduction in pore sizes for FLP@MIL-101(Cr) compared with pristine MIL-101(Cr), suggesting the successful anchoring of FLP molecules within the pores of the MOF. By this means, we expanded the solid foundation for the construction and applications of reusable porous FLP catalysts. Lately, we have also prepared and characterized P/B FLP@Nu-1000 catalysts that exhibited excellent performance for the hydrogenation of N-Heterocycles (Figure 4a–f).[56] Our seminal work attracted worldwide attention, and several groups have since applied the stepwise anchoring method to prepare MOF-based FLP catalysts.

Similarly, the replacement of Lewis base DABCO with 1,4-dioxane/*N*-dimethylethylenediamine (DMEDA),[44,55] and/or the exchange of BCF with mesityl borane MesB $(C_6F_5)_2$ in FLP@MIL-101(Cr) has been reported,[48] resulting in the preparation of several functional catalysts with diverging reactivities. Indeed, a multitude of SBUs belong to the category of Lewis acids which can be amenable to FLP chemistry. As an example, the Liang group[49,50] has reported the exploitation of Lewis acid SBUs to generate porous FLP catalysts. In their reports, they selected the Lewis base perylene-3,4,9,10-tetracarboxylic diimide (PDI) which was postsynthetically connected onto the organic linker of MIL-125(Ti)-NH_2 via an ammoniation reaction with the amine group, generating TiO_{5-x}-ligand-PDI FLPs. In addition to the activity of Lewis acid/Lewis base manipulation on FLPs, it is possible to incorporate extra functionality, particularly chirality. However, this remains challenging as the development of chiral frustrated Lewis pairs (CFLPs) for asymmetric catalysis is still in the infancy stage. As proof of concept, we have pioneered this idea of CFLP@MOFs by exploiting bifunctional bulky chiral Lewis bases post-synthetically grafted onto the walls of MOF pores at one site, leaving the other site to interact with an achiral bulky Lewis acid.[57,58] Such a demonstration could largely expand the library of CFLP catalysts, as well as provide new opportunities for asymmetric catalysis.

Enzymes have also been incorporated into the nanospaces of MOFs by chemical postmodification. The latest progress has been made by the Chen group,[60] offering a generalized defect generation strategy for enzyme immobilization in MOFs. Typically, the incorporation of guest molecules via postmodification requires guest molecules and MOF's pores to reach a size match. Based on the size evaluation of enzymes, the pore size should be larger than 3 nm in qualified MOFs, which is a serious limitation considering the required stability under enzyme-compatible conditions. To overcome this limitation, as well as avoid harsh synthetic conditions, it is imperative to develop a strategy applicable to MOFs regardless of pore size for the incorporation of enzymes. To this end, the Chen group[60] used an enzyme as the "macro ligand" to compete with traditional organic linkers in coordination with SBUs, the resultant generation of defects promotes the transportation of enzymes from the surface to the bulk. Specifically, the proof-of-concept paradigm was realized upon UIO-66, which was water- stable and possessed pore diameters (1.0 nm) smaller than that of the selected model enzyme: lipase (3.0 × 4.0 × 5.0 nm). To understand the immobilization process and mechanism, an in situ super-resolution imaging system (SIM) was applied to monitor the time-dependent distribution changes of the enzyme, referred to as a fluorescein isothiocyanate (FITC)-tagged lipase. Along with the time increase of immersing UIO-66 in lipase solution, SIM images revealed that the FITC-labeled enzymes began to embed in the outer layer of UIO-66 crystals and proceeded to occupy the interlayer. The successful accommodation of lipase by UIO-66 implied the emergence of large pores, attributed to the generation of defects during the enzyme immobilization process. The release of the organic linker and the observed coordination of lipase to the Zr sites using respective nuclear magnetic resonance (NMR) measurement and XPS spectra together confirm the successful incorporation of lipase by chemical post-modification induced defects generation.

Bottom-up construction

Although pore encapsulation and chemical postmodification methods can easily and efficiently incorporate active molecular species into MOFs, they are still largely influenced by the size of both host pores and carriers, as well as restrictions by reaction conditions. This could be supplemented by treating active molecular species as SBUs or organic ligands for bottom-up MOF synthesis, leading to functional MOF materials that incorporate/combine active components. Porphyrins are a type of well-known bioactive molecule, which also exhibit widespread applicability in contemporary materials and catalysis. In recent years, porphyrin MOFs have particularly been studied, thanks to facile preparations from the assembly of SBUs and custom-designed porphyrin ligands, among which tetrakis(4-carboxyphenyl)porphyrin (TCPP) is one of the most frequently used.[61–63] Even so, the combination of crystal engineering and add-on functionality at the porphyrin center have together generated a tremendous library of porphyrin MOFs, which serve as versatile catalysts. The Zhou group[64–66] has laid a solid foundation in this area and recently presented the mixed linker strategy to examine the crystal structure and the properties of porphyrin MOFs. To name a few, they applied the tetratopic linker TCPP and tritopic linkers

DOI: 10.31635/ccschem.024.202403909
Citation: *CCS Chem.* **2024**, 6, 1380–1402
Link to VoR: https://doi.org/10.31635/ccschem.024.202403909

such as 1,3,5-tris(4-carboxyphenyl)benzene (BTB) or 4,4′,4″-(2,4,6-trimethylbenzene-1,3,5-triyl)tribenzoate (TBTB) in conjunction with different metal clusters to produce two MOFs: $[(CH_3)_2NH_2]_4[Zn_4O]_4[Zn(TCPP)]_5[BTB]_{8/3}$ (PCN-137) and $[Zr_6(\mu_3\text{-}O)_4(\mu_3\text{-}OH)_4][TCPP][TBTB]_{8/3}$ (PCN-138).[64] Specifically, two combinations: (1) Zn_4O clusters (vertices), BTB (triangular faces), and TCPP (square faces), (2) Zr_6O clusters (vertices), TBTB (triangular faces) and TCPP (square faces) formed two types of Archimedean solids (rhombicuboctahedron and cuboctahedron, respectively), which accumulated to give rise to framework of PCN-137 as a 3D (3,4,7)-connected **qyc** net and framework of PCN-138 as a 3D (3,4,12)-connected **urr** net. This information was obtained from single-crystal X-ray diffraction studies. The phase purity of the as-prepared samples was examined by PXRD patterns which matched well with the simulated patterns. In another study, the structural difference was disclosed by merely changing the way the linkers were added.[65] The one-pot reaction of BTB, TCPP, and zirconium precursors yielded the three-dimensional PCN-134-3D, while the sequential synthesis provided a two-dimentional PCN-134-2D counterpart, undergoing a Zr-BTB nanosheets formation and a subsequent TCPP coordination. This work provided ideal platforms to investigate structure-property relationships of materials with different structures yet identical compositions. In 2021, the same group presented an exploration of porphyrin MOFs with tetratopic ligands of very similar size but with distinct photoelectronic properties.[66] This involved the usage of TCPP and TBAPy. In one strategy, the TCPP was selected as the linker and photoelectron acceptor to construct a two-dimensional TCPP-Zr-NS MOF which was modified by a photoelectron donor of TBAPy. Another strategy depicted a reverse way to obtain the material by preparing TBAPy-Zr-NS MOF first, then in coordination with TCPP. The Su group[67,68] has also contributed significantly to this area. Accordingly, they created bimetallic functionality based on porphyrin MOFs and fully exploited the synergistic effect. For instance, the decoration of Iridium species to TCPP yielded Ir-TCPP which served as the organic linker for Ir-PCN-222 synthesis. Subsequent introduction of Au into Ir-PCN-222 was conducted with the intention of improving the composite's reactivity and selectivity toward specific reactants.[67] Transmission electron microscopy (TEM) was employed to visualize the gold nanoparticle embedded in the Au@Ir-PCN-222 obtained, and the elemental mapping results revealed the existence and ordered distribution of both Ir and Au elements. To demonstrate the generality of this bimetallic strategy in porphyrin-based MOF systems and to seek catalysts of high efficiency and novel reactivity, they utilized a Pd-centered TCPP ligand and synthesized the corresponding Pd-PCN-222, which was anchored afterward with different spatially isolated single atoms (SAs), assisted by the connector of 4-aminobenzoic acid, offering a series of M-SAs@Pd-PCN-222-NH_2 (M = Pt, Ir, Au, and Ru) catalysts.[68] The presence and status of SAs were examined and confirmed by high-angle annular dark-field scanning transmission electron microscopy (HAADF-STEM), XANES, and EXAFS. It should be noted that the porphyrin ligand itself has long been adopted as a carrier of active sites. For example, the Wang group[69] reported the decoration of hollow-structured PCN-222 MOF with single or multiple components of single noble metal sites. The Lin group[70] prepared porphyrin-MOF starting from Ru_2 paddlewheel SBUs and organic linker TCPP with/without Zn^{II}-metalation. The Lan group[71,72] further contributed to well-defined and readily available polyoxometalate (POM) clusters, including Zn-ε-keggin $\{\varepsilon\text{-}PMo_8^{V}Mo_4^{VI}O_{40}Zn_4\}$ clusters which served as a type of reactive SBUs, and coordinated with diverse M-TCPP ligands to generate a library of POM-metalloporphyrin organic frameworks (PMOFs). The structure and photophysical characterization of PMOFs have been well presented (Figure 5a–d). Our group specializes in developing metal-metalloporphyrin frameworks (MMPFs) with custom-designed porphyrin linkers via crystal engineering to achieve unexpected performance in catalysis.[73,74] Lately, we successfully obtained MMPF-5 single crystals from a solvothermal reaction between 5,15-bis(3,5-dicarboxyphenyl)-10,20-bis(2,6-dibromophe-nyl)porphyrin (H_4dcdbp) and $MgCl_2$.[73] We anticipated that MMPF-5, which had a high-density of C-Br bonds throughout the framework, could serve as synthetic halogen capsules with binding pockets to realize value-added transformations akin to enzymes. Furthermore, a set of MMPFs was prepared to investigate how accessible coordination sites and tunable steric hindrance within the cavity of catalysts could affect their selectivity to both reagents and products.[61,74] In summary, the reports described above provide guidelines for the preparation of porphyrin MOFs and subtle changes that drastically diversify their applications.

Compared with porphyrins, the availability and synthetic ease of amino acids and peptides make them a promising component in MOF design and synthesis through a bottom-up construction approach. As a recent prototype, we reference the work of Guo et al.[75] in which the synthesized chiral organic molecules, derived from natural amino acids, including valine (Val)-, serine (Ser)-, and threonine (Thr), not only mimic privileged natural cinchona alkaloids at the single-chiral-site level with the expectation to realize superior chiral induction but also have been successfully used to synthesize corresponding chiral MOFs (Val-MOF, Ser-MOF, and Thr-MOF) with zinc precursors. The Pardo group[76] also developed chiral ligands H_2Me_2-(*S, S*)-serimox and H_2Me_2-(*S, S*)-Mecysmox, derived from amino acids L-serine and L-mecysteine, respectively. Considering the similarity of these two ligands, the synthesis of MOFs with each ligand and

DOI: 10.31635/ccschem.024.202403909
Citation: *CCS Chem.* **2024**, 6, 1380–1402
Link to VoR: https://doi.org/10.31635/ccschem.024.202403909

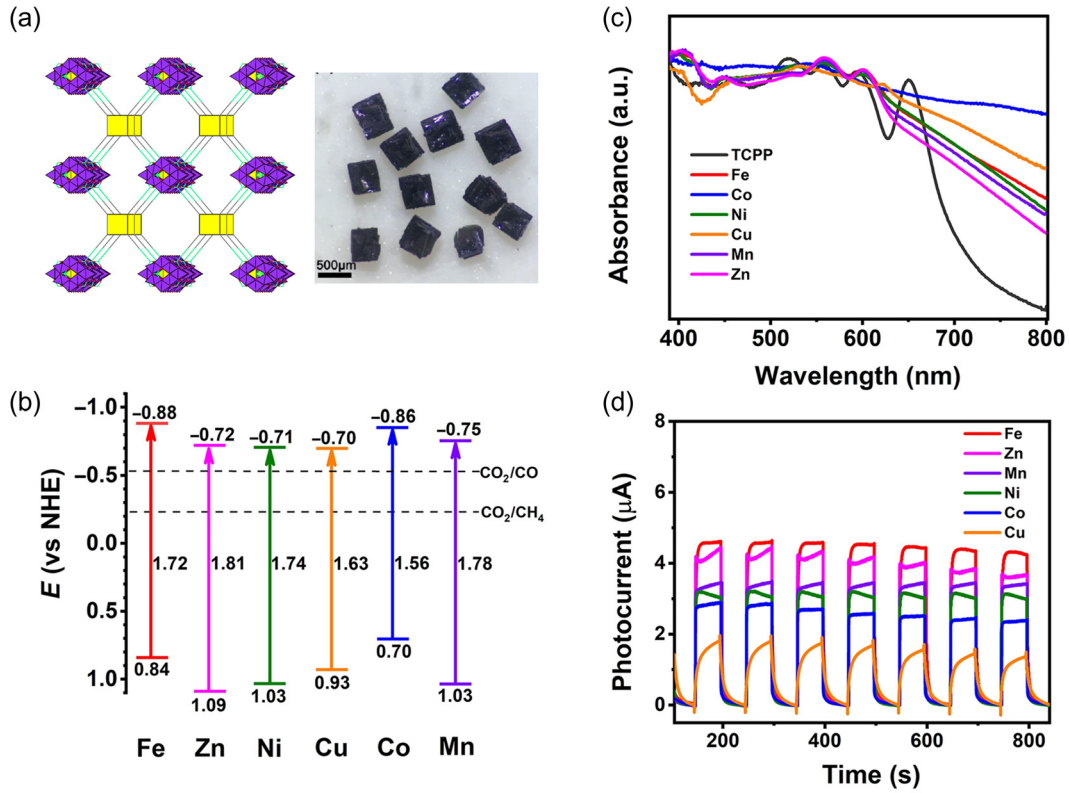

Figure 5 | *Featured characterizations of PMOF catalysts. (a) The scheme (left) and real crystal (right) of Fe-PMOF three-dimensional frameworks. (b) UV–visible diffuse reflection spectra for different PMOFs. (c) The bandgap determinations of different PMOFs suggest they are good catalyst candidates for photocatalytic CO_2 conversions. (d) Transient photocurrent curves of different PMOFs reveal that Fe-PMOF has the strongest charge separation efficiency. Reproduced with permission from ref 72. Copyright 2023 American Association for the Advancement of Science. PMOF, polyoxometalate-metalloporphyrin organic framework.*

mixed ligands of an equal percentage was attainable. This provided appreciable models for investigating how the host–guest interaction could affect the catalysis performance of multivariate MOFs.

The majority of progress incorporating proteins/enzymes within the framework of MOFs has been achieved via bottom-up construction (in situ coprecipitation/biomineralization). Without special pore-size limitations on both MOF host and protein/enzyme guest, bottom-up construction allows for facile preparation of composites via a one-pot reaction in the presence of protein/enzyme and precursors of MOF synthesis. In this minireview, we opt only for the latest progress on large-scale synthesis and exclusive characterization of MOF-protein/enzyme composites constructed through bottom-up strategy since this area has already been extensively reviewed with several prestigious works.[3–9] The chosen MOFs were typically among zeolitic imidazolate framework (ZIF),[77–92] microporous metal azolate framework (MAF),[93,94] and so on[95] families because they could crystallize from water in which proteins/enzymes could also maintain intrinsic structure and activity. The Chen group[96] has broadened the scope of the host by discovering a protein-assisted crystallization strategy through which a MOF of a new **sod** crystalline phase, namely ZPF-1, was obtained, along with the successful incorporation of the template protein. ZPF-1 could only be attained from pyrimidin-2-ol and zinc ions in the presence of proteins, without which nonporous MOF was afforded via traditional synthesis methods. This was attributed to the fact that the **sod** framework, preformed from zinc ions and the imidazole functional groups of histidine amino acid in selected proteins, could further expand to the resulting network with an excess pyrimidin-2-ol ligand. New techniques have also been applied to accelerate the synthesis of MOF-protein/enzyme biocomposites. The Falcaro group,[97] for example, has introduced the continuous-flow method to synthesize BSA@ZIF-8. In their work, the synchrotron time-resolved small-angle X-ray scattering (SAXS) was adopted to interrogate the nucleation, and growth of ZIF-8 upon the injection of the $Zn(OAc)_2$ and BSA-HmIM (2-methylimidazole) solutions. Amorphous particles were formed by BSA and HmIM coordinated to Zn^{2+} in the first 3 min and they subsequently convert into crystalline ZIF-8. In the flow reactor setup, a Y-mixer was used to mix

DOI: 10.31635/ccschem.024.202403909
Citation: *CCS Chem.* **2024**, 6, 1380–1402
Link to VoR: https://doi.org/10.31635/ccschem.024.202403909

$Zn(OAc)_2$ and BSA-HmIM solutions for amorphous particle formation, and a T-mixer was utilized to mix the preformed particles with ethanol, which accelerated the crystallization process. Furthermore, the particle size of the biocomposite could be tuned within a range of 40–100 nm by varying residence time prior to the introduction of ethanol. Previously, the Ren group[98] developed a microfluidic laminar flow synthesis of enzyme@ZIF-8 using a three-way mixing scheme because of the involvement of three species (Zn^{2+}, HmIM, and enzyme Cyt c) for the whole synthesis. Subsequently, they devised a double-Y-shaped microfluidic channel that could control the crystallization process by varying the time and concentration of the third species at the second Y to meet with the first two reactants, resulting in the synthesis of composites with defects, which could not be obtained in bulk solution under otherwise identical conditions. In terms of characterization of proteins/enzymes encapsulated in MOFs, in-situ SAXS techniques have recently taken appropriate advantages to unveil the dynamics of the encapsulation process, as well as to reveal the stability of confined enzymes at temperatures as high as 70 °C.[99] These studies have confirmed the successful encapsulation of enzymes by MOFs via the bottom-up strategy, as well as the synergistic effect MOF hosts could afford to improve the stability and performance of the enzyme guests.

Applying Catalysts of MOFs Housing Active Molecular Species for Catalysis

The utilization of the three major methods presented above facilitates the construction of numerous materials in the context of MOFs with active molecules. With active species of specific functionality in the porous region/framework of MOFs, as well as the synergies between MOFs and active species, these composite materials could drive a wide range of significant transformations, thereby propelling the industrialization of catalysis. In this section, we highlight some of the most exciting applications of catalyst@MOF materials, including asymmetric catalysis, CO_2 conversion, and biocatalysis.

Asymmetric reactions

The study of chiral molecules is directly relevant to human health since our body is composed of plentiful left-handed chiral substances, which exhibit distinct stereospecific pharmacochemical interactions with foreign chiral molecules. In pursuit of efficient synthesis and facile isolation of pure chiral molecules, asymmetric catalysis is the most efficient and sustainable method available. Asymmetric catalysis with the participation of bioactive molecules and/or molecular FLPs may alleviate the traditional reliance on noble metal active sites for activity and the tedious synthesis of privileged chiral ligands for selectivity. In this section we highlight innovative advancements in MOF-based asymmetric catalysis, conferring the intrinsic advantages of heterogeneous systems, as well as synergistic enhancement of efficiency, stability, and specificity relative to their homogeneous counterparts.

Asymmetric hydrogenation is a renowned reaction still full of potential for optimization of cost and atom efficiency, selectivity, and reaction conditions accompanied by catalyst innovation. Interestingly, a group of molecular CFLPs, designed based on computational results of hydrogenation thermodynamics and comprised of a simple chiral Lewis base and the bulky Lewis acid BCF, are active for asymmetric hydrogenation of imines, attaining a moderate yield and ee value in a homogenous manner.[57] Based upon this finding, our group has conceived up-to-date strategies for combining porous materials with active molecular species to contribute new types of catalysts for asymmetric hydrogenations. In our recent efforts, we have successfully synthesized a group of exclusive chiral catalysts using an operationally simple method of stepwise postmodification in which CFLPs were grafted onto open Cr^{III} metal sites of MIL-101(Cr) MOF dubbed CFLP@MOF. This novel material circumvented the issues of traditional catalysts, generally involving expensive noble metals and lengthy chiral ligand synthesis, as well as issues related to homogeneous systems including stability, recyclability, and product separation. Importantly, in stark contrast to the homogeneous analog, enhanced performance was achieved after the introduction of CFLPs into the nanospace of MOFs. This was attributed to the enriched FLP active sites and enforced stronger chiral environment within MOF porous regions, as well as the confinement effect in CFLP@MIL-101(Cr). In general optimization of catalysts and reaction conditions, the influence of different types and amounts of CFLP and the solvent effect on catalysts' performance were studied. CFLP4-0.75@MIL-101(Cr) performed the best among all tested catalysts in the hydrogenation of (E)-N,1-diphenylethan-1-imine with a yield of 97% and an ee value of 86% under 40 bar H_2 at room temperature in a toluene solution. This catalyst maintained superior performance in recycle tests over five consecutive runs, indicating the excellent recyclability of heterogeneous CFLP@MIL-101(Cr) catalysts. Furthermore, we found that CFLP4-0.75@MIL-101(Cr) was compatible with a wide substrate scope, yielding a diverse library of asymmetric hydrogenation products. This innovative demonstration has inspired work across multiple fields to combine porous materials and FLP chemistry, not only laying a solid foundation for the design and preparation of chiral catalysts but also foreseeing their applications in asymmetric hydrogenation and beyond, including under conditions incompatible with MOFs.

DOI: 10.31635/ccschem.024.202403909
Citation: *CCS Chem.* **2024**, 6, 1380–1402
Link to VoR: https://doi.org/10.31635/ccschem.024.202403909

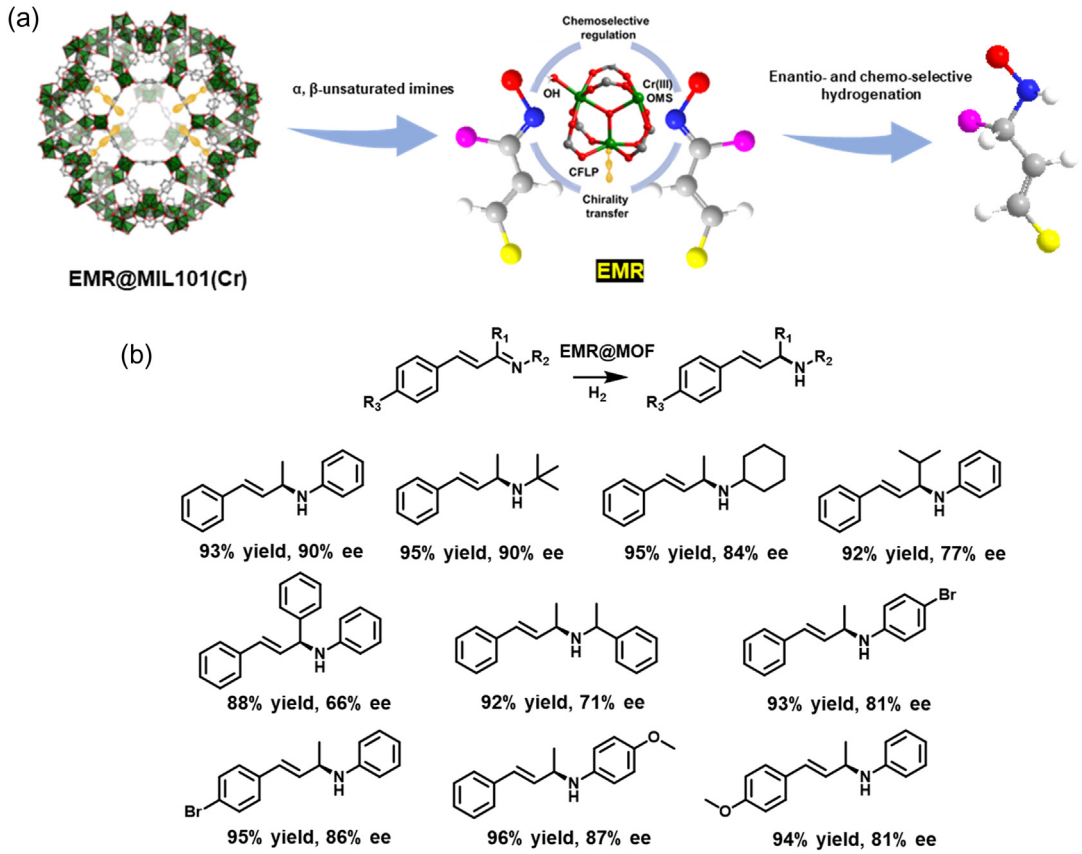

Figure 6 | *Catalysis performance of CFLP4-0.75@MIL-101(Cr) for asymmetric hydrogenation. (a) Schematic illustration of preparing EMR@MIL-101 for enantio- and chemoselective hydrogenation of α,β-unsaturated imine. (b) Catalytic performance of CFLP4-0.75@MIL-101(Cr) toward enantio- and chemoselective hydrogenation with different substrates. Reproduced with permission from ref 58. Copyright 2023 ACS Publications. CFLP, chiral frustrated Lewis pairs; EMR@MIL-101, enzyme-mimic region of the chromium terephthalate MOF (MIL = Matérial Institut Lavoisier), MOF, metal–organic framework.*

In another report, we further demonstrated chemoselectivity in addition to enantioselectivity in asymmetric hydrogenation by taking inspiration from nature to judiciously exploit the synergy between MOF and CFLP functionalities (Figure 6a).[58] Inspired by enzymes that could impart enantioselectivity with intrinsic strong chirality and might regulate another selectivity through second-sphere interactions with auxiliary groups in the vicinity of active centers, great progress has been made in mimicking enzymes for the design and preparation of catalysts to tackle challenging issues associated with multiple- and variable selectivity for significant reactions. Nonetheless, it remains a daunting task in heterogeneous systems. We pioneered the creation of an "enzyme-mimic region" (EMR) within the nanospace of a MOF (EMR@MOF) by grafting a CFLP onto the MOF pore wall and tailoring the vicinity of CFLP with auxiliary directing sites (ASs); the chiral nature of CFLP could impart enantioselectivity, and the ASs might regulate chemoselectivity via preferential orientation of substrate via secondary interactions reminiscent of enzymes. As a proof-of-concept study, asymmetric hydrogenation of α,β-unsaturated imines was selected because of its potential in synthesizing pharmacologically valuable chiral β-unsaturated amines. To this end, CFLPs consisting of functional chiral Lewis bases and the bulky Lewis acid $MesB(C_6F_5)_2$ were introduced into MIL-101(Cr), which had open Cr^{III} metal sites and hydroxyl groups at abundant SBUs, resulting in the preparation of EMR@MIL-101 (Cr) catalysts. It was found that molecular CFLP4 itself could enable the hydrogenation of α,β-unsaturated imine despite indistinguishable chemoselectivity between C=C/C=N group. Auspiciously, the MOF-supported CFLP4-0.75@MIL-101(Cr) afforded the production of chiral β-unsaturated amine with noticeably higher yield (95%) and ee value (88%). In contrast, MIL-101(Cr) was catalytically inactive toward hydrogenation. Additionally, mechanically mixing MIL-101(Cr) and CFLP4 only led to catalysis performance on par with CFLP4. These results indicated the importance of CFLP and the tailored local environment of MOF SBUs in mediating enantioselectivity and chemoselectivity. The study on how the

DOI: 10.31635/ccschem.024.202403909
Citation: *CCS Chem.* **2024**, 6, 1380–1402
Link to VoR: https://doi.org/10.31635/ccschem.024.202403909

type and density of EMR affected its catalysis performance suggested that CFLP4-0.75@MIL-101(Cr) at 7.5 mol% was the optimal candidate among the investigated catalysts. A solvent effect test screening three common solvents CH_2Cl_2, toluene, and CH_3CN, revealed nonpolar, non-coordinating toluene as superior, likely, a consequence of its lack of interaction with the polar directing groups. In addition, EMR@MIL-101(Cr) exhibited excellent recyclability and broad substrate scope enabling chemo- and enantioselective hydrogenation for a diverse assortment of substrates (Figure 6b). Since SBUs of MIL-101(Cr) have been reported to selectively activate C=O/C=N over C=C groups, we sought to probe the interaction between catalyst and substrate by measuring the IR spectra of CFLP4-0.75@MIL-101(Cr) samples before and after immersion into liquid (2E,3E)-*N*-(*tert*-butyl)-4-phenylbut-3-en-2-imine. Characteristic peaks of MIL-101(Cr), CFLP4, and substrate were observed and reasonably assigned. Notable changes have been seen after the introduction of the substrate to the catalyst, including ν(C=N) redshifted (from 1679 to 1669 cm^{-1}), and the appearance of a broad feature was noted at ~3350 cm^{-1}. These observations were due to the formation of imine-metal complex and formation of H-bonding between C=N and hydroxyl groups, respectively, revealing preferable interaction of C=N over C=C in α,β-unsaturated imine with MOF SBUs. Complementary results led to the proposal of a reaction mechanism reminiscent of enzymes, showcasing second-sphere interactions between the substrate and SBUs-mediated chemoselectivity in-pore CFLP active sites, activating H_2 in a classic heterolytic cleavage manner, as well as hydrogen bonding and π–π interactions regulating chirality transfer from the catalyst to the product. This work, which demonstrated the construction of selective catalysts based on MOFs has been extended to other heterogeneous systems, inspiring asymmetric hydrogenation in other porous materials, as well as other significant reactions.

Guo et al.[75] embedded platinum nanoparticles (1.8 nm) as hydrogenation active sites in chiral MOFs (Val-MOF, Ser-MOF, and Thr-MOF) by solvent reduction. Under the same reaction conditions: 1.3 mmol of Pt, 10 μL of ethyl pyruvate, 2 mL of solvent, 4 MPa H_2, a reaction time of 12 h, and a reaction temperature of 25 °C, resulted Pt-*l(d)*-Val-MOF, Pt-*l(d)*-Ser-MOFs, and Pt-*l(d)*-Thr-MOF catalyzed hydrogenation of ethyl pyruvate with ascending conversions though a detectable ee value could only be obtained in case of Pt-*l(d)*-Thr-MOF. Using Pt-*l*-Thr-MOF as the catalyst, solvent polarity variation from methanol to isopropanol and toluene could substantially tune the performance. When the reaction proceeded in methanol, a 24% ee value was obtained albeit a 40.9% conversion. While low-polarity solvents such as isopropanol and toluene significantly promoted the reaction conversion, it also resulted in a steep decrease in the value of the product. The increase in reaction time with Pt-*l*-Thr-MOF as the catalyst led to 99.5% conversion and 23.9% ee value. Furthermore, conducting the reaction under a lower reaction temperature (0 °C) resulted in an increased ee value of 27.3%, yet at the cost of decreased conversion (30.2%). Nearly complete conversion of ethyl pyruvate via hydrogenation evidenced the efficiency of Pt nanoparticles, and the successful chiral induction was attributed to the effective formation of hydrogen bonding interactions between MOF and substrate, as well as the presence of chiral centers adjacent to binding sites. This work provided a good reference for the implementation of asymmetric catalysis based on MOF catalysts and intrigued important strategies for reaction optimization.

The synthesized chiral L-valim-UiO-FeCl, L-alaim-UiO-FeCl, and L-leucim-UiO-FeCl from the Manna group[35] have been examined in asymmetric hydrogenation of ketones via a sequential hydrosilylation and hydrolysis process. All three catalysts showed high efficiency in the quantitative conversion of acetophenone to the final hydrogenation product, while L-valim-UiO-FeCl achieved the best ee value of 92%. The distinct enantioselectivity of these chiral catalysts could be explained by the discrete steric and electronic properties of different amino entities present in each respective MOF catalyst. L-valim-UiO-FeCl was found to transform various ketones to corresponding alcohols with high conversions and ee values. It had a higher performance than its homogeneous counterpart and could reach a turnover number (TON) of 10,000. This revealed the advantageous efficiency of a single-site catalyst and the unexpected cooperation of its host–guest structure. A standard leaching test showed that the leaching was less than 0.5% Fe after 10 runs. A mechanistic investigation uncovered the reaction route starting from the activation of L-valim-UiO-FeCl by $LiCH_2SiMe_3$, resulting in the generation of L-valim-UiO-Fe-(CH_2SiMe_3), which subsequently reacts with $(OEt)_2MeSiH$ under the in-pore chiral environment which favored an S-pathway and hydrosilylation product. They presented an indispensable example for developing single-site base-metal catalysts that highlighted the benefit of site-isolation of catalytically active species confined within the nanospace of a MOF.

CO_2 transformations

CO_2 is of tremendous abundance on the earth because of its inevitable production from myriad sources. This raises considerable concern as CO_2 is a major contributor to the greenhouse effect. Thus, the transformation of CO_2 from readily available sources into value-added commodities represents an attractive strategy toward the sustainable use of carbon-based fuels. In practice, a multitude of promising catalysts have been devised to implement this strategy, aimed at industrialization. MOFs housing active molecular species have also been widely constructed as

DOI: 10.31635/ccschem.024.202403909
Citation: *CCS Chem.* **2024**, 6, 1380–1402
Link to VoR: https://doi.org/10.31635/ccschem.024.202403909

catalysts and applied toward the exclusive transformation of CO_2 into valuable chemicals such as CO, methanol, cyclic carbonates, formamides, HCOOH, and so on, under mild conditions.

According to the report of the Lan group,[71] M-PMOFs (M = Co, Fe, Ni, and Zn) were applied for CO_2 electroreduction. The exceptional stability of M-PMOFs with respect to temperature, oxygen, and $KHCO_3$ aqueous solution laid the foundation for their electrochemical studies. Co-PMOF was mainly investigated considering its superior total current density (38.9 mA cm^{-2}), smaller onset potential (−0.35 V), and overpotential (0.24 V) compared with other samples, evidenced by Linear sweep voltammetry (LSV) curves in CO_2-saturated 0.5M $KHCO_3$ (pH = 7.2) solution. The gas chromatography analysis revealed that CO and H_2 were the major products, and there was no liquid product. As for the selectivity of Co-PMOF for the CO_2 reduction reaction (CO_2RR), the maximum CO Faradaic efficiency (FE_{CO}) attained at −0.8 V was 98.7%, which was notably high. Tafel slope calculation yielded 98 mV dec^{-1} for Co-PMOF, notably smaller than other samples. The favorable formation of CO with Co-PMOF was attributed to more efficient charge transfer and a larger active surface in the catalysis process. These findings were supported by the results obtained from electrochemical double-layer capacitance (C_{dl}) and electrochemical impedance spectroscopy (EIS) measurements, as Co-PMOF had a larger C_{dl} value (12.17 mF cm^{-2}) and smaller charge transfer resistance (9.83 Ω). A long-time durability test with Co-PMOF confirmed its composition, structure, and capacity maintenance for 36 h. The combination of POM and TCPP in a well-defined structure realized cooperation with each part to achieve an impressive performance. Moreover, the same group applied M-PMOF (M = Fe^{III}, Zn^{II}, Ni^{II}, Cu^{II}, Co^{II}, and Mn^{II}) constructed from M-TCPP and reductive POM for photo- and electrocatalytic CO_2 reductions, obtaining high methane production of 922 micromoles per gram and 92.1% FE_{CO} with Fe-PMOF, respectively.[72] Mechanistic investigations implied that photosensitive iron-TCPP moieties could absorb light energy and transfer photogenerated electrons to the POM cluster for methane generation, while the abundant electrons flowed to the center of iron-TCPP for CO formation under the applied electric field.

Given that porphyrin-based MOFs have the tunable redox properties of porphyrin species and the modifiable reactive/functional sites of MOFs, various strategies have been adopted to improve their CO_2RR performance. For instance, replacing one type of aromatic C–H with C-NH_2 at TCPP drastically enhanced the electroreduction performance of FE_{CO} from 47.4% to 99.4%.[100] The reason lied in the fact that local amino groups served as hydrogen-bonding donors to stabilize the Co-CO_2 adduct intermediate and prevented the formation of the Co-H_2O adduct, leading to the promotion of CO generation and compression of hydrogen evolution. Besides, acceleration of electron transfer efficiency was effective in enhancing the CO_2RR performance. Catalysts with two dimensions could enhance conductivity and expose high-density active sites. Recently, the Chen group[101] successfully prepared ultrathin two-dimensional Co-based porphyrin porous organic layers, which exhibited a current of over 200 mA in a membrane electrode assembly reactor and maintained near-unity CO selectivity over 20 h in CO_2 electrolysis. In parallel, Dong et al.[102] mixed PCN-222 (Fe) with carbon black (mass ratio = 1:2) to increase conductivity, reaching a maximum of 91% FE_{CO}.

Chemical conversion of CO_2 to liquid products such as methanol is also desirable. Recently, the Zhang group[103] reported the utilization of porphyrin-MOF Ir-PCN-222 for selective thermocatalytic conversion of CO_2 to methanol via the hydrosilylation route, achieving 99% conversion and 99% selectivity under a low CO_2 concentration (15% CO_2 and 85% N_2). Porphyrin entities constructed within Ir-PCN-222 of a **csq** topology promoted the MOF's affinity to CO_2, activated by Ir sites coordination by porphyrin at N atoms for the hydrosilylation process in which a concentration balance between CO_2 and hydrosilanes inside MOF contributed to afford excellent selectivity.

The transformation of CO_2 to cyclic carbonates has also been well documented. Continuous progress has been made with MOFs housing active molecular species as catalysts. Recently, porphyrin-based MOFs including Rh^{III},[104] Ir^{III},[104] and Fe^{III}[105] centered TCPP molecules have been demonstrated to be good heterogeneous catalysts for efficient thermocatalytic fixation of CO_2 into cyclic carbonates. In pursuit of a more sustainable method, a visible-light-driven chemical transformation has also been reported with Mg-centered porphyrin MOF which displayed superior activity over thermal catalysis conditions,[106] resulting from efficient ligand-to-metal charge transfer that lowered the activation barrier of CO_2 for its cycloaddition with epoxides. In addition, bimetallic modification at the center of the porphyrin ring rendered PCN-224 a better catalyst to achieve a higher yield of cyclic carbonates,[107] a consequence of activation of both CO_2 and epoxides via balanced acidic/basic site concentrations.

Coupling CO_2 with readily available amine feedstocks has also gained widespread attention. In our own efforts, a robust metal–organic cage (MOC), constructed from a $Cp_3Zr_3O(OH)_3$ cluster and Lewis acidic boronic linker, could efficiently catalyze CO_2 fixation into diamines with the assistance of hydrosilanes in-situ, the in-pore bulky boronic Lewis acid could form active FLP sites with Lewis basic diamines added to the reaction solution.[108] FLP@MOC activated both hydrosilane and CO_2 to accelerate the production of benzimidazoles from a number of diamines with good to excellent yields. This work offered yet another example of the development of heterogeneous FLP catalysts for the activation of small molecules.

DOI: 10.31635/ccschem.024.202403909
Citation: *CCS Chem.* **2024**, 6, 1380–1402
Link to VoR: https://doi.org/10.31635/ccschem.024.202403909

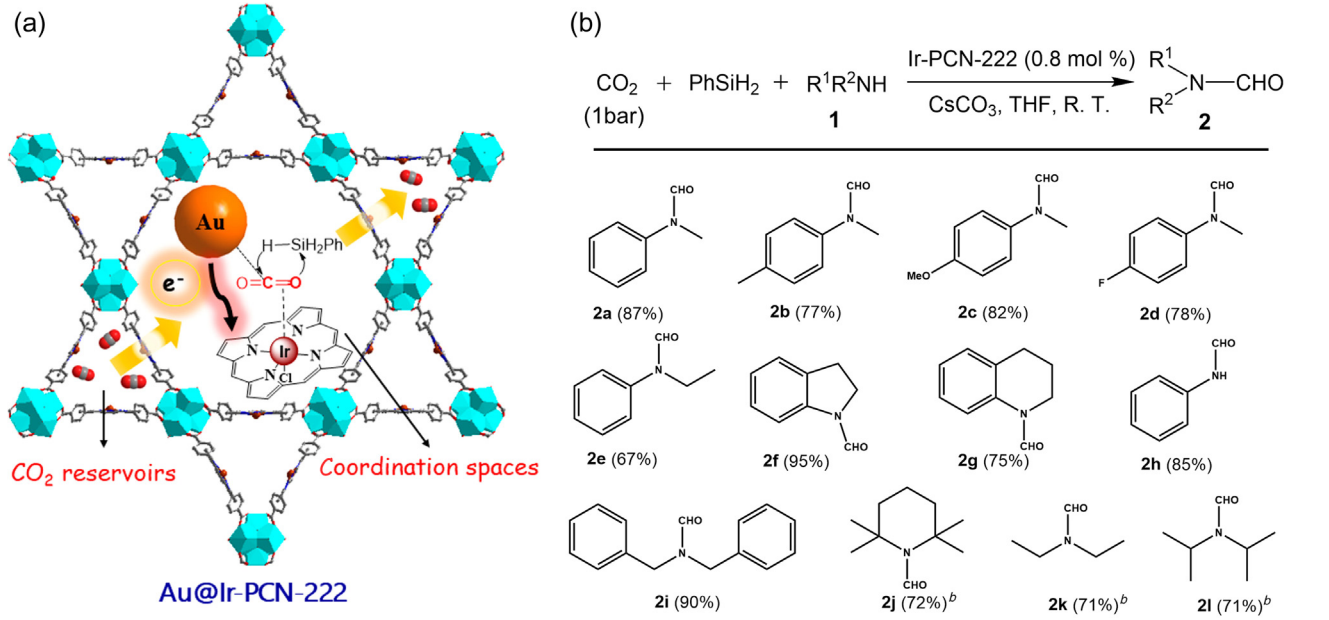

Figure 7 | *Catalysis performance of Au@porphyrin-Ir-PCN-222 for CO_2 transformation. (a) Schematic illustration of CO_2 adsorption, diffusion, and activation in the inner cavities of Au@Ir-PCN-222. (b) The catalysis performance of producing formamides via CO_2 reduction and aminolysis. Reproduced with permission from ref 67. Copyright 2020 ACS Publications.*

The Su group[67] has been particularly impressive by successfully implementing formamides synthesis from secondary amine, CO_2, and $PhSiH_3$ with Au@Ir-PCN-222 as the heterogeneous catalyst (Figure 7a,b). Under atmospheric pressure and ambient temperature, Ir-PCN-222 gave an 89% yield and a good selectivity (98:2) for the formamide product after 24 h, while replacing Ir with Rh, Ru, or Pd led to substantially reduced performance. Interestingly, the introduction of different metal nanoparticles to Ir-PCN-222 substantially enhanced the performance of M@Ir-PCN-222 (M = Ir, Pd, Pt, Au) composites, among which Au@Ir-PCN-222 was found to be the most efficient, producing formamide with 90% yield and 91:9 selectivity in only 2 h. As rationale, it was proposed that Au^0 ($5d^{10}6s^1$) was prone to transfer electrons to Ir-porphyrin units, thereby increasing the interactions with CO_2 molecules in addition to enhancing adsorption. However, Ir-porphyrin was confirmed to be the active site in Au@Ir-PCN-222, as no reaction occurred using Au nanoparticles as the catalyst. This work provided guidelines for both CO_2 adsorption and activation by MOF catalysts with an integration of catalytically active porphyrins and other functional units.

Biocatalysis

The utilization of enzyme-mimicking catalysts for biocatalysis is a straightforward application. Peroxidation of organic molecules is one of the most widely used model reactions to examine the performance of various catalysts with the addition of hydrogen peroxide. To check the activity of MP-11 encapsulated in Tb-mesoMOF, we used resultant MP-11@Tb-mesoMOF as the catalyst for 3,5-dit-butyl-catechol (DTBC) peroxidation in the presence of 10 mM H_2O_2 (methanol solution) at room temperature.[20] Separately, MP-11 and Tb-mesoMOF could only drive the transformation to a low extent, as MP-11 began to aggregate within 3 min and Tb-mesoMOF exhibited poor activity. In contrast, a significantly higher yield (48.7%) was obtained using the catalyst of MP-11@Tb-mesoMOF. This result indicated the successful encapsulation of MP-11 into Tb-mesoMOF to construct a microperoxidase that achieved enhanced stability and performance. In comparison to the mesoporous silicate and alumosilicate matrices, with uniform cylindrical pores widely studied in enzyme immobilization such as multi-chip-module (MCM), MP-11@MCM-41 has also been prepared and used for peroxidation tests. Although it exhibited a faster reaction rate of 3.57×10^{-5} mM/s, MP-11@MCM-41 could only reach 17% conversion because the catalyst was deactivated as a consequence of leaching MP-11 during the reaction process. This indicated that the selection of a matrix with proper pore size and robustness is of great importance. Considering the convenience of conducting and tracing peroxidation, research groups across the world have since adopted the same methods to test the activity of peroxidase@MOF systems (Figure 8a–d).[3-8] In addition, this work has inspired other encapsulated enzymatic reactions, thanks to the immense diversity and variety of enzymes. Examples

DOI: 10.31635/ccschem.024.202403909
Citation: *CCS Chem.* **2024**, 6, 1380–1402
Link to VoR: https://doi.org/10.31635/ccschem.024.202403909

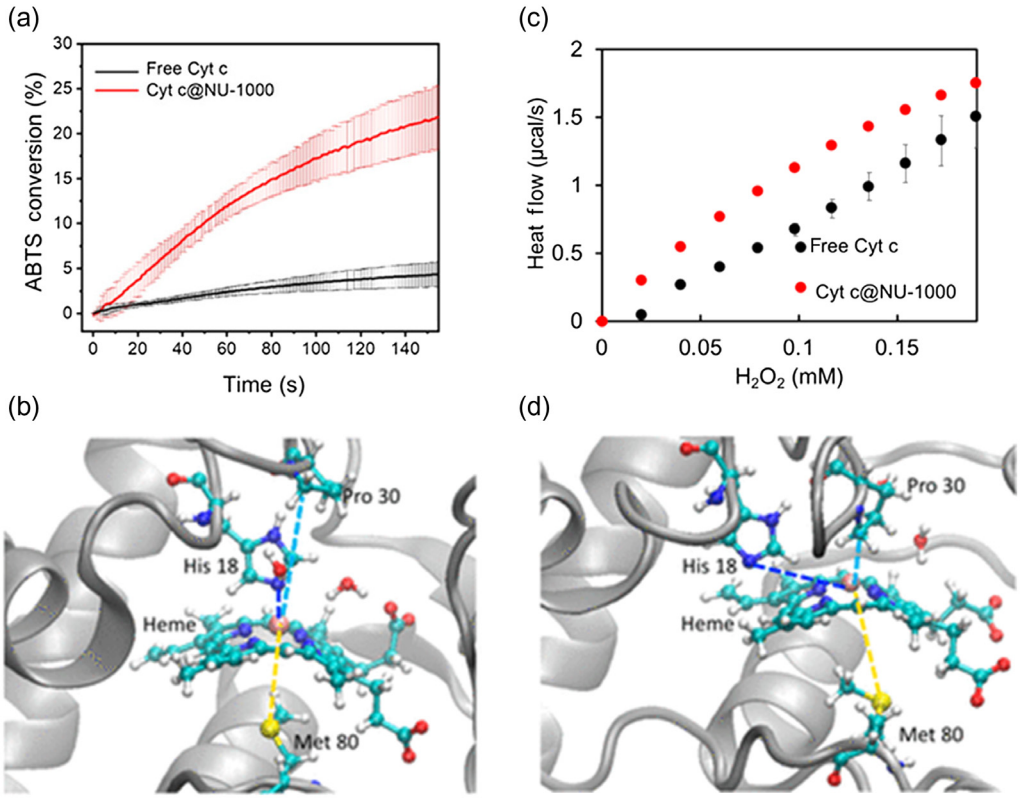

Figure 8 | *Catalysis performance of Cyt c@NU-1000 in biocatalysis. (a) The H_2O_2 oxidation performance catalyzed by Cyt c and Cyt c@NU-1000 shows that the latter has a notably higher efficiency. (b) The analyzed calorimetric data for the multiple injections of H_2O_2 into reaction solutions containing Cyt c or Cyt c@NU-1000 indicate that Cyt c@NU-1000 shows a higher rate because of more heat release. The configurational difference of Cyt C in water (c) and inside NU-1000 (d), namely different coordination of the Cyt c heme active sites with changed distribution of P(D), N (His 18), S (Met 80), and C (Pro 30), leading to distinct performance. Reproduced with permission from ref 26. Copyright 2020 ACS Publications.*

include selective peptide bond cleavage using proteases,[109] and hydrolysis of 4-nitrophenyl acetate using esterases,[110] to name just a few.

Other catalysis categories

The combination of MOF and active molecular species endows rich reactivity of the resultant catalysts. In addition to asymmetric transformations, CO_2 conversions, and biocatalysis, MOF encapsulated catalysts have been presented in the context of hydrogen evolution,[68,70,111–114] C–C and C–X coupling reactions,[115] C–H activation,[116] CH_4 oxidation,[117] and so on, have also been implemented with exciting results, promising to meet the ever-growing demands and requirements of chemical industries toward supplying pharmaceuticals, energy, commodity chemicals, and other advanced materials.

Conclusion and Outlook

In the pursuit of heterogenous catalysts achieving high specificity, high selectivity, and high efficiency like enzymes, different types of active molecular species such as enzymes, peptides, amino acids, porphyrins, and FLPs have been grafted or encapsulated into MOF hosts. This strategy could not only improve the stability but also synergistically enrich the reactivity of guest species, thereby leading to enhanced performance, as well as stability. The modular nature of MOF design and synthesis, together with the widely available sources of active molecular species yielded facile and flexible combinations through multiple methods. In this minireview, we summarized three approaches, namely pore encapsulation, chemical postmodification, and bottom-up construction. By far, pore encapsulation has been the principal method used to combine each unit by simply mixing them in a liquid solution. Nevertheless, the size match between the MOF host and molecular guest plays a crucial role in affording high encapsulation efficiency and low leaching possibility of guest molecules. Moreover, there remains a significant opportunity to elucidate the fundamental interactions and dynamics between MOF, encapsulated molecules, and substrate, as well as reveal the conformation of encapsulated molecules

DOI: 10.31635/ccschem.024.202403909
Citation: *CCS Chem.* **2024**, 6, 1380–1402
Link to VoR: https://doi.org/10.31635/ccschem.024.202403909

through instrumental and conceptual innovation. The prominent chemical postmodification method provides a powerful strategy to exert molecular level control with high accuracy on the nanoenvironment of a MOF to achieve groundbreaking advances. Nonetheless, judicious selection regarding the chemical functionality of each component is crucial to ensure compatibility of robustness and the pore size of the MOF host must also be considered. These requirements have inspired the development of spectroscopic methodologies to detect subtle changes resulting from the formation of chemical bonds/interactions and have intrigued the design and synthesis of diverse functional MOFs. Finally, the bottom-up construction has largely overcome the issue of size match between each unit, albeit resulting in a rising complexity in SBUs/organic linker design and synthesis, as well as challenging structural determination of resultant MOFs. We anticipate that in the future, the limitations on both MOFs and active molecular species will be considerably mitigated with the assistance of artificial intelligence for morphological/compositional screening and structural prediction.

Upon the acquisition of numerous catalysts of MOF housing active molecular species, their applications for significant transformations have been particularly reviewed. The intrinsic chirality of bioactive molecules incorporated in MOFs made them particularly advantageous for heterogeneous asymmetric catalysis. The progress of successful implementation of highly valuable transformations including asymmetric hydrogenation, particularly, empowered by single-site base metal in exceptional efficiency, as converged attention from across broad fields. Notably, recyclable catalysts prepared by the introduction of CFLPs into MOFs have opened new opportunities for asymmetric hydrogenation and more. Interestingly, despite the obvious trajectory, the direct utilization of MOFs housing enzymes as catalysts for asymmetric reactivity has not been sufficiently probed, perhaps due to the difficulty in selecting and purifying an enzyme of small size and proper stability. At this stage, the construction of peptides@MOFs[118] as well as the biomimetic frameworks[119] for asymmetric reactions may remain feasible choices. We anticipate that fruitful endeavors will continue rapidly to satisfy the rising demand for chiral substances, and the utility of MOFs housing active molecular species will be one of the most promising catalyst paradigms with the potential for realizing new-to-nature reactivities. Of particularly critical importance, the functional catalysts reviewed herein competent for the catalysis of CO_2 conversion strategies have the potential to provide solutions for remediating issues of ever-increasing global CO_2 emissions. Although most of the reported catalysts still largely rely on external energy input such as heat/electricity to achieve reasonable efficiency, sustainable plans, seeking photoinduced/enzymatic routes are also underway. In terms of active molecular species used in the construction of composite MOF catalysts for CO_2 conversion, porphyrins will continue to be a promising platform thanks to their diverse and finely tunable qualities. Meanwhile, FLP@MOF is an emerging paradigm, which may prove to be a valuable candidate for selective CO_2 conversion under mild conditions. Furthermore, opportunity abounds in the establishment of novel catalytic systems to convert CO_2 into multicarbon products and realize net-zero carbon-based fuel production, as the major product of CO_2 reduction remains the undesirable CO in most current systems. Therefore, explicit mechanistic investigation, which, in turn, aids rational, task-specific catalyst design by combining active molecular species and MOFs,[120] is imperative.

To date, fruitful progress has been made in a multitude of reaction systems with catalysts of active molecular species incorporated in MOFs, yet the design and application of these catalysts are still in their infancy. On one hand, efforts must be made to improve the stability of catalysts resistant to highly acidic/basic reaction conditions. On the other hand, in the pursuit of target applications, efforts need to pivot from maximizing the activity of individual units towards the complementary design of host–guest cooperative reactivity to realize more important and/or complex transformations. Additionally, the continued development of earth-abundant element catalysts (e.g. main-group and base-metal elements) should be prioritized to yield practical and scalable materials to meet rising demand.[121] In short, this minireview summarizes the construction of recyclable catalysts achieved through the introduction of active molecular species into MOF structures for enhanced catalytic performance over the past five years; we hope the corresponding outlook provided also inspires the reader to contribute and expand this area in new and exciting directions.

Conflict of Interest

There is no conflict of interest to report.

Acknowledgments

This work was supported by the Robert A. Welch Foundation (grant no. B-0027).

References

1. Wang, K.-Y.; Zhang, J.; Hsu, Y.-C.; Lin, H.; Han, Z.; Pang, J.; Yang, Z.; Liang, R.-R.; Shi, W.; Zhou, H.-C. Bioinspired Framework Catalysts: From Enzyme Immobilization to Biomimetic Catalysis. *Chem. Rev.* **2023**, *123*, 5347–5420.
2. Dai, S.; Funk, L.-M.; Von Pappenheim F. R.; Sautner, V.; Paulikat, M.; Schröder, B.; Uranga, J.; Mata, R. A.; Tittmann, K. Low-Barrier Hydrogen Bonds in Enzyme Cooperativity. *Nature* **2019**, *573*, 609–613.

DOI: 10.31635/ccschem.024.202403909
Citation: *CCS Chem.* **2024**, 6, 1380–1402
Link to VoR: https://doi.org/10.31635/ccschem.024.202403909

3. An, H.; Li, M.; Gao, J.; Zhang, Z.; Ma, S.; Chen, Y. Incorporation of Biomolecules in Metal-Organic Frameworks for Advanced Applications. *Coordin. Chem. Rev.* **2019**, *384*, 90–106.
4. Cai, H.; Huang, Y.-L.; Li, D. Biological Metal-Organic Frameworks: Structures, Host-Guest Chemistry and Bio-Applications. *Coordin. Chem. Rev.* **2019**, *378*, 207–221.
5. Drout, R. J.; Robison, L.; Farha, O. K. Catalytic Applications of Enzymes Encapsulated in Metal-Organic Frameworks. *Coordin. Chem. Rev.* **2019**, *381*, 151–160.
6. Huang, S.; Kou, X.; Shen, J.; Chen, G.; Ouyang, G. "Armor-Plating" Enzymes with Metal-Organic Frameworks (MOFs). *Angew. Chem. Int. Ed.* **2020**, *59*, 8786–8798.
7. Duan, W.; Zhao, Z.; An, H.; Zhang, Z.; Cheng, P.; Chen, Y.; Huang, H. State-of-the-Art and Prospects of Biomolecules: Incorporation in Functional Metal-Organic Frameworks. *Top. Curr. Chem.* **2019**, *377*, 34.
8. Liang, S.; Wu, X.-L.; Xiong, J.; Zong, M.-H.; Lou, W.-Y. Metal-Organic Frameworks as Novel Matrices for Efficient Enzyme Immobilization: An Update Review. *Coordin. Chem. Rev.* **2020**, *406*, 213149.
9. Bindra, A. K.; Wang, D.; Zhao, Y. Metal-Organic Frameworks Meet Polymers: From Synthesis Strategies to Healthcare Applications. *Adv. Mater.* **2023**, *35*, e2300700.
10. Holm, R. H.; Lo, W. Structural Conversions of Synthetic and Protein-Bound Iron-Sulfur Clusters. *Chem. Rev.* **2016**, *116*, 13685–13713.
11. Cui, J. D.; Jia, S. R. Optimization Protocols and Improved Strategies of Cross-Linked Enzymes Aggregates Technology: Current Development and Future Challenges. *Crit. Rev. Biotechnol.* **2015**, *35*, 15–28.
12. Pascanu, V.; González Miera, G.; Inge, A. K.; Martín-Matute, B. Metal-Organic Frameworks as Catalysts for Organic Synthesis: A Critical Perspective. *J. Am. Chem. Soc.* **2019**, *141*, 7223–7234.
13. Xu, W.; Gu, W.; Du, D.; Lin, Y.; Zhu, C. Atomic-Level Design of Metalloenzyme-like Active Pockets in Metal-Organic Frameworks for Bioinspired Catalysis. *Chem. Soc. Rev.* **2024**, *53*, 137–162.
14. Lam, J.; Szkop, K. M.; Mosaferi, E.; Stephan, D. W. FLP Catalysis: Main Group Hydrogenations of Organic Unsaturated Substrates. *Chem. Soc. Rev.* **2019**, *48*, 3592–3612.
15. Jupp, A.; Stephan, D. W. New Directions for Frustrated Lewis Pair Chemistry. *Trends Chem.* **2019**, *1*, 35–48.
16. Stephan, D. W. Catalysis, FLPs, and Beyond. *Chem* **2020**, *6*, 1520–1526.
17. Stephan, D. W. Diverse Uses of the Reaction of Frustrated Lewis Pair (FLP) with Hydrogen. *J. Am. Chem. Soc.* **2021**, *143*, 20002–20014.
18. Zhang, Y.; Lan, P.; Martin, K.; Ma, S. Porous Frustrated Lewis Pair Catalysts: Advances and Perspective. *Chem. Catal.* **2022**, *2*, 439–457.
19. Feng, L.; Wang, K.-Y.; Lv, X.-L.; Yan, T.-H.; Zhou, H.-C. Hierarchically Porous Metal-Organic Frameworks: Synthetic Strategies and Applications. *Natl. Sci. Rev.* **2020**, *7*, 1743–1758.
20. Lykourinou, V.; Chen, Y.; Wang, X.-S.; Meng, L.; Hoang, T.; Ming, L.-J.; Musselman, R. L.; Ma, S. Immobilization of MP-11 into a Mesoporous Metal-Organic Framework, MP-11@mesoMOF: A New Platform for Enzymatic Catalysis. *J. Am. Chem. Soc.* **2011**, *133*, 10382–10385.
21. Chen, Y.; Lykourinou, V.; Vetromile, C.; Hoang, T.; Ming, L.-J.; Larsen, R. W.; Ma, S. How Can Proteins Enter the Interior of a MOF? Investigation of Cytochrome c Translocation into a MOF Consisting of Mesoporous Cages with Microporous Windows. *J. Am. Chem. Soc.* **2012**, *134*, 13188–13191.
22. Chen, Y.; Han, S.; Li, X.; Zhang, Z.; Ma, S. Why Does Enzyme Not Leach from Metal-Organic Frameworks (MOFs)? Unveiling the Interactions Between an Enzyme Molecule and a MOF. *Inorg. Chem.* **2014**, *53*, 10006–10008.
23. Wang, X.; He, L.; Summer, J.; Qian, S.; Zhang, Q.; O'Neill, H.; Mao, Y.; Chen, C.; Al-Enizi, A. M.; Nafady, A.; Ma, S. Spatially Confined Protein Assembly in Hierarchical Mesoporous Metal-Organic Framework. *Nat. Commun.* **2023**, *14*, 973.
24. Li, P.; Modica, J. A.; Howarth, A. J.; Vargas L. E.; Moghadam, P. Z.; Snurr, R. Q.; Mrksich, M.; Hupp, J. T.; Farha, O. K. Toward Design Rules for Enzyme Immobilization in Hierarchical Mesoporous Metal-Organic Frameworks. *Chem* **2016**, *1*, 154–169.
25. Chen, Y.; Li, P.; Modica, J. A.; Drout, R. J.; Farha, O. K. Acid-Resistant Mesoporous Metal-Organic Framework Toward Oral Insulin Delivery: Protein Encapsulation, Protection, and Release. *J. Am. Chem. Soc.* **2018**, *140*, 5678–5681.
26. Chen, Y.; Jiménez-Ángeles, F.; Qiao, B.; Krzyaniak, M. D.; Sha, F.; Kato, S.; Gong, X.; Buru, C. T.; Chen, Z.; Zhang, X.; Gianneschi, N. C.; Wasielewski, M. R.; Olvera de la Cruz, M.; Farha, O. K. Insights into the Enhanced Catalytic Activity of Cytochrome c When Encapsulated in a Metal-Organic Framework. *J. Am. Chem. Soc.* **2020**, *142*, 18576–18582.
27. Sha, F.; Xie, H.; Son, F. A.; Kim, K. S.; Gong, W.; Su, S.; Ma, K.; Wang, X.; Wang, X.; Farha, O. K. Rationally Tailored Mesoporous Hosts for Optimal Protein Encapsulation. *J. Am. Chem. Soc.* **2023**, *145*, 16383–16390.
28. Li, P.; Moon, S.-Y.; Guelta, M. A.; Harvey, S. P.; Hupp, J. T.; Farha, O. K. Encapsulation of a Nerve Agent Detoxifying Enzyme by a Mesoporous Zirconium Metal-Organic Framework Engenders Thermal and Long-Term Stability. *J. Am. Chem. Soc.* **2016**, *138*, 8052–8055.
29. Chen, Y.; Li, P.; Zhou, J.; Buru, C. T.; Đorđević, L.; Li, P.; Zhang, X.; Cetin, M. M.; Stoddart, J. F.; Stupp, S. I.; Wasielewski, M. R.; Farha, O. K. Integration of Enzymes and Photosensitizers in a Hierarchical Mesoporous Metal-Organic Framework for Light-Driven CO_2 Reduction. *J. Am. Chem. Soc.* **2020**, *142*, 1768–1773.
30. Greifenstein, R.; Ballweg, T.; Hashem, T.; Gottwald, E.; Achauer, D.; Kirschhöfer, F.; Nusser, M.; Brenner-Weiß, G.; Sedghamiz, E.; Wenzel, W.; Mittmann, E.; Rabe, K. S.; Niemeyer, C. M.; Franzreb, M.; Wöll, C. MOF-Hosted Enzymes for Continuous Flow Catalysis in Aqueous and Organic Solvents. *Angew. Chem. Int. Ed.* **2022**, *61*, e202117144.
31. Feng, D.; Liu, T.-F.; Su, J.; Bosch, M.; Wei, Z.; Wan, W.; Yuan, D.; Chen, Y.-P.; Wang, X.; Wang, K.; Lian, X.; Gu, Z.-Y.; Park, J.; Zou, X.; Zhou, H.-C. Stable Metal-Organic Frameworks Containing Single-Molecule Traps for Enzyme Encapsulation. *Nat. Commun.* **2015**, *6*, 5979.

DOI: 10.31635/ccschem.024.202403909
Citation: *CCS Chem.* **2024**, 6, 1380–1402
Link to VoR: https://doi.org/10.31635/ccschem.024.202403909

32. Gkaniatsou, E.; Sicard, C.; Ricoux, R.; Benahmed, L.; Bourdreux, F.; Zhang, Q.; Serre, C.; Mahy, J.-P.; Steunou, N. Enzyme Encapsulation in Mesoporous Metal-Organic Frameworks for Selective Biodegradation of Harmful Dye Molecules. *Angew. Chem. Int. Ed.* **2018**, *57*, 16141–16146.
33. Ahmad, R.; Rizaldo, S.; Gohari, M.; Shanahan, J.; Shaner, S. E.; Stone, K. L.; Kissel, D. S. Buffer Effects in Zirconium-Based UiO Metal-Organic Frameworks (MOFs) That Influence Enzyme Immobilization and Catalytic Activity in Enzyme/MOF Biocatalysts. *ACS Omega* **2023**, *8*, 22545–22555.
34. Gheorghe, A.; Strudwick, B.; Dawson, D. M.; Ashbrook, S. E.; Woutersen, S.; Dubbeldam, D.; Tanase, S. Synthesis of Chiral MOF-74 Frameworks by Post-Synthetic Modification by Using an Amino Acid. *Chem. Eur. J.* **2020**, *26*, 13957–13965.
35. Newar, R.; Akhtar, N.; Antil, N.; Kumar, A.; Shukla, S.; Begum, W.; Manna, K. Amino Acid-Functionalized Metal-Organic Frameworks for Asymmetric Base-Metal Catalysis. *Angew. Chem. Int. Ed.* **2021**, *60*, 10964–10970.
36. Antil, N.; Akhtar, N.; Newar, R.; Begum, W.; Kumar, A.; Chauhan, M.; Manna, K. Chiral Iron(II)-Catalysts within Valinol-Grafted Metal-Organic Frameworks for Enantioselective Reduction of Ketones. *ACS Catal.* **2021**, *11*, 10450–10459.
37. Canivet, J.; Bernoud, E.; Bonnefoy, J.; Legrand, A.; Todorova, T. K.; Quadrelli, E. A.; Mellot-Draznieks, C. Synthetic and Computational Assessment of a Chiral Metal-Organic Framework Catalyst for Predictive Asymmetric Transformation. *Chem. Sci.* **2020**, *11*, 8800–8808.
38. Niu, Z.; Bhagya Gunatilleke, W. D. C.; Sun, Q.; Lan, P. C.; Perman, J.; Ma, J.-G.; Cheng, Y.; Aguila, B.; Ma, S. Metal-Organic Framework Anchored with a Lewis Pair as a New Paradigm for Catalysis. *Chem* **2018**, *4*, 2587–2599.
39. Shyshkanov, S.; Nguyen, T. N.; Chidambaram, A.; Stylianou, K. C.; Dyson, P. J. Frustrated Lewis Pair-Mediated Fixation of CO_2 Within a Metal-Organic Framework. *Chem. Commun.* **2019**, *55*, 10964–10967.
40. Shyshkanov, S.; Nguyen, T. N.; Ebrahim, F. M.; Stylianou, K. C.; Dyson, P. J. In Situ Formation of Frustrated Lewis Pairs in a Water-Tolerant Metal-Organic Framework for the Transformation of CO_2. *Angew. Chem. Int. Ed.* **2019**, *58*, 5371–5375.
41. Li, X.; Deng, Q.; Yu, L.; Gao, R.; Tong, Z.; Lu, C.; Wang, J.; Zeng, Z.; Zou, J.-J.; Deng, S. Double-Metal Cyanide as an Acid and Hydrogenation Catalyst for the Highly Selective Ring-Rearrangement of Biomass-Derived Furfuryl Alcohol to Cyclopentenone Compounds. *Green Chem.* **2020**, *22*, 2549–2557.
42. He, Y.; Li, C.; Chen, X.-B.; Shi, Z.; Feng, S. Visible-Light-Responsive UiO-66(Zr) with Defects Efficiently Promoting Photocatalytic CO_2 Reduction. *ACS Appl. Mater. Interfaces* **2022**, *14*, 28977–28984.
43. Chen, M.; Wang, M.; Ji, M. Design and Synthesis of Heterogeneous Frustrated Lewis Pairs for Hydrogenation: From Molecular Immobilization to Defects Engineering. *ChemCatChem* **2024**, e202301472.
44. Chen, M.; Xu, H.; Zhao, H.; Bai, W.; Ji, M. Selective Hydrogenation of Carbon-Carbon Double Bond Catalyzed by FLP-MOFs. *Micropor. Mesopor. Mater.* **2023**, *359*, 112633.
45. Cui, H.; Liao, X.; Ren, Y.; Zhou, Y.; Xiao, J.; Deng, R.; Lv, Y.; Liu, H.; Liu, P.; Yang, H. Highly Selective Transfer Hydrogenation of α,β-Unsaturated Aldehydes by Frustrated Lewis Pairs (FLPs) on Oxygen-Defect-Rich Co_3O_4@NC. *J. Catal.* **2023**, *428*, 115126.
46. Cui, H.; Zhong, L.; Liao, X.; Hao, F.; Xiong, W.; Liu, H.; Luo, H.; Liu, P.; Lv, Y. Highly Efficient Chemoselective Hydrogenation of Unsaturated Aldehydes Catalyzed by Hydrophobically Modified Core-Shell Defective ZIFs: Frustrated Lewis Pair Catalysis. *J. Catal.* **2023**, *420*, 23–43.
47. Dhakshinamoorthy, A.; Asiri, A. M.; Garcia, H. New Opportunities in Metal-Organic Framework Catalysis: From Bifunctional to Frustrated Lewis Pairs Catalysis. *Chem. Eur. J.* **2023**, *29*, e202204016.
48. Niu, Z.; Zhang, W.; Lan, P. C.; Aguila, B.; Ma, S. Promoting Frustrated Lewis Pairs for Heterogeneous Chemoselective Hydrogenation via the Tailored Pore Environment within Metal-Organic Frameworks. *Angew. Chem. Int. Ed.* **2019**, *58*, 7420–7424.
49. Liang, R.; Wang, S.; Xia, Y.; Wu, L.; Huang, R.; He, Z. Frustrated Lewis Pair Boosting Photocatalytic Antibacterial Activity on PDI-Bridged Bimetallic UiO-66-NH_2. *Dalton Trans.* **2023**, *52*, 6813–6822.
50. Wang, S.; Xia, Y.; Yan, G.; Chen, M.; Wang, X.; Wu, L.; Liang, R. PDI Bridged MIL-125(Ti)-NH_2 Heterojunction with Frustrated Lewis Pairs: A Promising Photocatalyst for Cr(VI) Reduction and Antibacterial Application. *Appl. Catal. B: Environ.* **2022**, *317*, 121798.
51. Liang, Y.; Zhang, Z.; Su, X.; Feng, X.; Xing, S.; Liu, W.; Huang, R.; Liu, Y. Coordination Defect-Induced Frustrated Lewis Pairs in Polyoxo-Metalate-Based Metal-Organic Frameworks for Efficient Catalytic Hydrogenation. *Angew. Chem. Int. Ed.* **2023**, *62*, e202309030.
52. Melillo, A.; Franconetti, A.; Alvaro, M.; Ferrer, B.; Garcia, H. Metal Nodes of Metal-Organic Frameworks Can Activate Molecular Hydrogen. *Chem. Eur. J.* **2023**, *29*, e202202625.
53. Ng, B. K. Y.; Zhou, Z.-J.; Liu, T.-T.; Yoskamtorn, T.; Li, G.; Wu, T. S.; Soo, Y.-L.; Wu, X.-P.; Tsang, S. C. E. Photo-Induced Active Lewis Acid-Base Pairs in a Metal-Organic Framework for H_2 Activation. *J. Am. Chem. Soc.* **2023**, *145*, 19312–19320.
54. Xu, H.; Song, X.; Chen, M.; Bai, W.; Ji, M. Rigid Confined Space in Frustrated Lewis Pair/MOF Catalyst: Highly Regioselective Reduction of α, β-Unsaturated Carbonyl Compounds. *J. Catal.* **2023**, *421*, 342–350.
55. Xu, H.; Song, X.; Chen, M.; Bai, W.; Zhang, J.; Ji, M. Frustrated Lewis Pairs Bridged by Water and Immobilized in a Metal-Organic Framework as a Recyclable Transfer Hydrogenation Nanocatalyst. *ACS Appl. Nano Mater.* **2023**, *6*, 5255–5263.
56. Xu, Z.-M.; Hu, Z.; Huang, Y.; Bao, S.-J.; Niu, Z.; Lang, J.-P.; Al-Enizi, A. M.; Nafady, A.; Ma, S. Introducing Frustrated Lewis Pairs to Metal-Organic Framework for Selective Hydrogenation of N-Heterocycles. *J. Am. Chem. Soc.* **2023**, *145*, 14994–15000.
57. Zhang, Y.; Chen, S.; Al-Enizi, A. M.; Nafady, A.; Tang, Z.; Ma, S. Chiral Frustrated Lewis Pair@Metal-Organic Framework as a New Platform for Heterogeneous Asymmetric

DOI: 10.31635/ccschem.024.202403909
Citation: *CCS Chem.* **2024**, 6, 1380–1402
Link to VoR: https://doi.org/10.31635/ccschem.024.202403909

Hydrogenation. *Angew. Chem. Int. Ed.* **2023**, *62*, e202213399.
58. Zhang, Y.; Jiang, Y.; Nafady, A.; Tang, Z.; Al-Enizi, A. M.; Tan, K.; Ma, S. Incorporation of Chiral Frustrated Lewis Pair into Metal-Organic Framework with Tailored Microenvironment for Heterogeneous Enantio- and Chemoselective Hydrogenation. *ACS Cent. Sci.* **2023**, *9*, 1692–1701.
59. Zhang, Y.; Guo, J.; VanNtta, P.; Jiang, Y.; Phipps, J.; Roknuzzaman, R.; Rabaâ, H.; Kui, T.; AlShahrani, T.; Ma, S. Metal-Free Heterogeneous Asymmetric Hydrogenation of Olefins Promoted by Chiral Frustrated Lewis Pair Framework. *J. Am. Chem. Soc.* **2024**, *146*, 979–987.
60. Feng, Y.; Shi, R.; Yang, M.; Zheng, Y.; Zhang, Z.; Chen, Y. A Dynamic Defect Generation Strategy for Efficient Enzyme Immobilization in Robust Metal-Organic Frameworks for Catalytic Hydrolysis and Chiral Resolution. *Angew. Chem. Int. Ed.* **2023**, *62*, e202302436.
61. Gao, W.-Y.; Chrzanowski, M.; Ma, S. Metal-Metalloporphyrin Frameworks: A Resurging Class of Functional Materials. *Chem. Soc. Rev.* **2014**, *43*, 5841–5866.
62. Feng, L.; Wang, K.-Y.; Joseph, E.; Zhou, H.-C. Catalytic Porphyrin Framework Compounds. *Trends Chem.* **2020**, *2*, 555–568.
63. Zhang, X.; Wasson, M. C.; Shayan, M.; Berdichevsky, E. K.; Ricardo-Noordberg, J.; Singh, Z.; Papazyan, E. K.; Castro, A. J.; Marino, P.; Ajoyan, Z.; Chen, Z.; Islamoglu, T.; Howarth, A. J.; Liu, Y.; Majewski, M. B.; Katz, M. J.; Mondloch, J. E.; Farha, O. K. A Historical Perspective on Porphyrin-Based Metal-Organic Frameworks and Their Applications. *Coord. Chem. Rev.* **2021**, *429*, 213615.
64. Qiu, Y.-C.; Yuan, S.; Li, X.-X.; Du, D.-Y.; Wang, C.; Qin, J.-S.; Drake, H. F.; Lan, Y.-Q.; Jiang, L.; Zhou, H.-C. Face-Sharing Archimedean Solids Stacking for the Construction of Mixed-Ligand Metal-Organic Frameworks. *J. Am. Chem. Soc.* **2019**, *141*, 13841–13848.
65. Wang, Y.; Feng, L.; Pang, J.; Li, J.; Huang, N.; Day, G. S.; Cheng, L.; Drake, H. F.; Wang, Y.; Lollar, C.; Qin, J.; Gu, Z.; Lu, T.; Yuan, S.; Zhou, H.-C. Photosensitizer-Anchored 2D MOF Nanosheets as Highly Stable and Accessible Catalysts toward Artemisinin Production. *Adv. Sci.* **2019**, *6*, 1802059.
66. Cai, P.; Xu, M.; Meng, S.-S.; Lin, Z.; Yan, T.; Drake, H. F.; Zhang, P.; Pang, J.; Gu, Z.-Y.; Zhou, H.-C. Precise Spatial-Designed Metal-Organic-Framework Nanosheets for Efficient Energy Transfer and Photocatalysis. *Angew. Chem. Int. Ed.* **2021**, *60*, 27258–27263.
67. Liu, J.; Fan, Y.-Z.; Zhang, K.; Zhang, L.; Su, C.-Y. Engineering Porphyrin Metal-Organic Framework Composites as Multifunctional Platforms for CO_2 Adsorption and Activation. *J. Am. Chem. Soc.* **2020**, *142*, 14548–14556.
68. Mo, Q.; Zhang, L.; Li, S.; Song, H.; Fan, Y.; Su, C.-Y. Engineering Single-Atom Sites into Pore-Confined Nanospaces of Porphyrinic Metal-Organic Frameworks for the Highly Efficient Photocatalytic Hydrogen Evolution Reaction. *J. Am. Chem. Soc.* **2022**, *144*, 22747–22758.
69. He, T.; Chen, S.; Ni, B.; Gong, Y.; Wu, Z.; Song, L.; Gu, L.; Hu, W.; Wang, X. Zirconium-Porphyrin-Based Metal-Organic Framework Hollow Nanotubes for Immobilization of Noble-Metal Single Atoms. *Angew. Chem. Int. Ed.* **2018**, *57*, 3493–3498.
70. Lan, G.; Zhu, Y. Y.; Veroneau, S. S.; Xu, Z.; Micheroni, D.; Lin, W. Electron Injection from Photoexcited Metal-Organic Framework Ligands to Ru_2 Secondary Building Units for Visible-Light-Driven Hydrogen Evolution. *J. Am. Chem. Soc.* **2018**, *140*, 5326–5329.
71. Wang, Y.-R.; Huang, Q.; He, C.-T.; Chen, Y.; Liu, J.; Shen, F.-C.; Lan, Y.-Q. Oriented Electron Transmission in Polyoxometalate-Metalloporphyrin Organic Framework for Highly Selective Electroreduction of CO_2. *Nat. Commun.* **2018**, *9*, 4466.
72. Huang, Q.; Niu, Q.; Li, X.-F.; Liu, J.; Sun, S.-N.; Dong, L.-Z.; Li, S.-L.; Cai, Y.-P.; Lan, Y.-Q. Demystifying the Roles of Single Metal Site and Cluster in CO_2 Reduction via Light and Electric Dual-Responsive Polyoxometalate-Based Metal-Organic Frameworks. *Sci. adv.* **2022**, *8*, eadd5598.
73. Zhang, W.; Nafady, A.; Shan, C.; Wojtas, L.; Chen, Y.-S.; Cheng, Q.; Zhang, X. P.; Ma, S. Functional Porphyrinic Metal-Organic Framework as a New Class of Heterogeneous Halogen-Bond-Donor Catalyst. *Angew. Chem. Int. Ed.* **2021**, *60*, 24312–24317.
74. Zhang, W.; Lu, Z.; Wojtas, L.; Chen, Y.-S.; Baker, A. A.; Liu, Y.-S.; Al-Enizi, A. M.; Nafady, A.; Ma, S. Kinetic Control via Binding Sites within the Confined Space of Metal Metalloporphyrin-Frameworks for Enhanced Shape-Selectivity Catalysis. *Angew. Chem. Int. Ed.* **2023**, *62*, e202304303.
75. Guo, J.; Duan, Y.; Liu, Y.; Li, H.; Zhang, Y.; Long, C.; Wang, Z.; Yang, Y.; Zhao, S. The Biomimetic Engineering of Metal-Organic Frameworks with Single-Chiral-Site Precision for Asymmetric Hydrogenation. *J. Mater. Chem. A* **2022**, *10*, 6463–6469.
76. Negro, C.; Sanz-Navarro, S.; Leyva-Pérez, A.; Armentano, D.; Ferrando-Soria, J.; Pardo, E. Exploring the Role of Amino Acid-Derived Multivariate Metal-Organic Frameworks as Catalysts in Hemiketalization Reactions. *Inorg. Chem.* **2023**, *62*, 7353–7359.
77. Chen, G.; Huang, S.; Kou, X.; Wei, S.; Huang, S.; Jiang, S.; Shen, J.; Zhu, F.; Ouyang, G. A Convenient and Versatile Amino-Acid-Boosted Biomimetic Strategy for the Nondestructive Encapsulation of Biomacromolecules within Metal-Organic Frameworks. *Angew. Chem. Int. Ed.* **2019**, *58*, 1463–1467.
78. Du, Y.; Gao, J.; Liu, H.; Zhou, L.; Ma, L.; He, Y.; Huang, Z.; Jiang, Y. Enzyme@Silica Nanoflower@Metal-Organic Framework Hybrids: A Novel Type of Integrated Nanobiocatalysts with Improved Stability. *Nano Res.* **2018**, *11*, 4380–4389.
79. Pan, Y.; Li, H.; Farmakes, J.; Xiao, F.; Chen, B.; Ma, S.; Yang, Z. How Do Enzymes Orient When Trapped on Metal-Organic Framework (MOF) Surfaces? *J. Am. Chem. Soc.* **2018**, *140*, 16032–16036.
80. Chen, S.-Y.; Lo, W.-S.; Huang, Y.-D.; Si, X.; Liao, F. S.; Lin, S.-W.; Williams, B. P.; Sun, T.-Q.; Lin, H.-W.; An, Y.; Sun, T.; Ma, Y.; Yang, H.-C.; Chou, L.-Y.; Shieh, F.-K.; Tsung, C.-K. Probing Interactions Between Metal-Organic Frameworks and Free-standing Enzymes in a Hollow Structure. *Nano Lett.* **2020**, *20*, 6630–6635.
81. Guo, J.; Yang, L.; Gao, Z.; Zhao, C.; Mei, Y.; Song, Y.-Y. Insight of MOF Environment-Dependent Enzyme Activity

DOI: 10.31635/ccschem.024.202403909
Citation: *CCS Chem.* **2024**, 6, 1380–1402
Link to VoR: https://doi.org/10.31635/ccschem.024.202403909

via MOFs-in-Nanochannels Configuration. *ACS Catal.* **2020**, *10*, 5949–5958.
82. Li, Q.; Pan, Y.; Li, H.; Alhalhooly, L.; Li, Y.; Chen, B.; Choi, Y.; Yang, Z. Size-Tunable Metal-Organic Framework-Coated Magnetic Nanoparticles for Enzyme Encapsulation and Large-Substrate Biocatalysis. *ACS Appl. Mater. Interfaces* **2020**, *12*, 41794–41801.
83. Li, Y.-M.; Yuan, J.; Ren, H.; Ji, C.-Y.; Tao, Y.; Wu, Y.; Chou, L.-Y.; Zhang, Y.-B.; Cheng, L. Fine-Tuning the Micro-Environment to Optimize the Catalytic Activity of Enzymes Immobilized in Multivariate Metal-Organic Frameworks. *J. Am. Chem. Soc.* **2021**, *143*, 15378–15390.
84. Tang, H.; Wang, H.; Du, J.; Zhao, D.; Cao, M.; Li, Y. Intrinsic Catalytic Activities from Single Enzyme@Metal-Organic Frameworks by Using a Stochastic Collision Electrochemical Technique. *J. Phys. Chem. Lett.* **2021**, *12*, 5443–5447.
85. Jiao, R.; Pang, Y.; Yang, D.; Li, Z.; Lou, H. Boosting Hydrolysis of Cellulose at High Temperature by beta-Glucosidase Induced Metal-Organic Framework In-Situ Co-Precipitation Encapsulation. *ChemSusChem* **2022**, *15*, e202201354.
86. Jordahl, D.; Armstrong, Z.; Li, Q.; Gao, R.; Liu, W.; Johnson, K.; Brown, W.; Scheiwiller, A.; Feng, L.; Ugrinov, A.; Mao, H.; Chen, B.; Quadir, M.; Li, H.; Pan, Y.; Yang, Z. Expanding the "Library" of Metal-Organic Frameworks for Enzyme Biomineralization. *ACS Appl. Mater. Interfaces* **2022**, *14*, 51619–51629.
87. Liang, J.; Bin Zulkifli, M. Y.; Yong, J.; Du, Z.; Ao, Z.; Rawal, A.; Scott, J. A.; Harmer, J. R.; Wang, J.; Liang, K. Locking the Ultrasound-Induced Active Conformation of Metalloenzymes in Metal-Organic Frameworks. *J. Am. Chem. Soc.* **2022**, *144*, 17865–17875.
88. Man, T.; Xu, C.; Liu, X.-Y.; Li, D.; Tsung, C.-K.; Pei, H.; Wan, Y.; Li, L. Hierarchically Encapsulating Enzymes with Multi-Shelled Metal-Organic Frameworks for Tandem Biocatalytic Reactions. *Nat. Commun.* **2022**, *13*, 305.
89. Tu, Y.; Li, H.; Tu, T.; Zhang, Q. Lamellar Enzyme-Metal-Organic Framework Composites Enable Catalysis on Large Substrates. *CCS Chem.* **2022**, *4*, 872–879.
90. Babaei, H.; Ghobadi Nejad, Z.; Yaghmaei, S.; Farhadi, F. Co-Immobilization of Multi-Enzyme Cascade System into the Metal-Organic Frameworks for the Removal of Bisphenol A. *Chem. Eng. J.* **2023**, *461*, 142050.
91. Yan, X.; Su, D.; Li, H.; Zhao, X.; Liu, X.; Liu, F.; Sun, P.; Lu, G. Ultrasensitive Plasmonic Immunosensor Based on Hierarchically Porous Metal-Organic Framework-Engineered Enzyme Catalysts. *Adv. Funct. Mater.* **2023**, *33*, 2215192.
92. Cai, G.; Ding, M.; Wu, Q.; Jiang, H.-L. Encapsulating Soluble Active Species into Hollow Crystalline Porous Capsules Beyond Integration of Homogeneous and Heterogeneous Catalysis. *Natl. Sci. Rev.* **2020**, *7*, 37–45.
93. Liang, W.; Xu, H.; Carraro, F.; Maddigan, N. K.; Li, Q.; Bell, S. G.; Huang, D. M.; Tarzia, A.; Solomon, M. B.; Amenitsch, H.; Vaccari, L.; Sumby, C. J.; Falcaro, P.; Doonan, C. J. Enhanced Activity of Enzymes Encapsulated in Hydrophilic Metal-Organic Frameworks. *J. Am. Chem. Soc.* **2019**, *141*, 2348–2355.
94. Xu, Y.; Liu, S. Y.; Liu, J.; Zhang, L.; Chen, D.; Chen, J.; Ma, Y.; Zhang, J.-P.; Dai, Z.; Zou, X. In Situ Enzyme Immobilization with Oxygen-Sensitive Luminescent Metal-Organic Frameworks to Realize "All-in-One" Multifunctions. *Chem. Eur. J.* **2019**, *25*, 5463–5471.
95. Hsu, P.-H.; Chang, C.-C.; Wang, T.-H.; Lam P. K.; Wei, M.-Y.; Chen, C.-Y.; Chou, L.-Y.; Shieh, F.-K. Rapid Fabrication of Biocomposites by Encapsulating Enzymes into Zn-MOF-74 via a Mild Water-Based Approach. *ACS Appl. Mater. Interfaces* **2021**, *13*, 52014–52022.
96. Wang, H.; Han, L.; Zheng, D.; Yang, M.; Andaloussi, Y. H.; Cheng, P.; Zhang, Z.; Ma, S.; Zaworotko, M. J.; Feng, Y.; Chen, Y. Protein-Structure-Directed Metal-Organic Zeolite-like Networks as Biomacromolecule Carriers. *Angew. Chem. Int. Ed.* **2020**, *59*, 6263–6267.
97. Carraro, F.; Williams, J. D.; Linares-Moreau, M.; Parise, C.; Liang, W.; Amenitsch, H.; Doonan, C.; Kappe, C. O.; Falcaro, P. Continuous-Flow Synthesis of ZIF-8 Biocomposites with Tunable Particle Size. *Angew. Chem. Int. Ed.* **2020**, *59*, 8123–8127.
98. Hu, C.; Bai, Y.; Hou, M.; Wang, Y.; Wang, L.; Cao, X.; Chan, C.-W.; Sun, H.; Li, W.; Ge, J.; Ren, K. Defect-Induced Activity Enhancement of Enzyme-Encapsulated Metal-Organic Frameworks Revealed in Microfluidic Gradient Mixing Synthesis. *Sci. Adv.* **2020**, *6*, eaax5785.
99. Murty, R.; Bera, M. K.; Walton, I. M.; Whetzel, C.; Prausnitz, M. R.; Walton, K. S. Interrogating Encapsulated Protein Structure within Metal-Organic Frameworks at Elevated Temperature. *J. Am. Chem. Soc.* **2023**, *145*, 7323–7330.
100. Wang, Y.; Huang, N.-Y.; Wang, H.-Y.; Zhang, X.-W.; Huang, J.-R.; Liao, P.-Q.; Chen, X.-M.; Zhang, J.-P. Local Weak Hydrogen Bonds Significantly Enhance CO_2 Electroreduction Performances of a Metal-Organic Framework. *CCS Chem.* **2023**, *5*, 145–151.
101. Zhang, W.; Liu, S.; Yang, Y.; Qi, H.; Xi, S.; Wei, Y.; Ding, J.; Wang, Z.-J.; Li, Q.; Liu, B.; Chen, Z. Exclusive Co-N_4 Sites Confined in Two-dimensional Metal-Organic Layers Enabling Highly Selective CO_2 Electroreduction at Industrial-Level Current. *Angew. Chem. Int. Ed.* **2023**, *62*, e202219241.
102. Dong, B.-X.; Qian, S.-L.; Bu, F.-Y.; Wu, Y.-C.; Feng, L.-G.; Teng, Y.-L.; Liu, W.-L.; Li, Z.-W. Electrochemical Reduction of CO_2 to CO by a Heterogeneous Catalyst of Fe-Porphyrin-Based Metal-Organic Framework. *ACS Appl. Energy Mater.* **2018**, *1*, 4662–4669.
103. Chen, C.; Mo, Q.; Huang, Y.; Zhang, L. Selective Reduction of CO_2 to Methanol via Hydrosilylation Boosted by a Porphyrinic Metal-Organic Framework. *ACS Catal.* **2023**, *13*, 6837–6845.
104. Liu, J.; Fan, Y.-Z.; Li, X.; Xu, Y.-W.; Zhang, L.; Su, C.-Y. Catalytic Space Engineering of Porphyrin Metal-Organic Frameworks for Combined CO_2 Capture and Conversion at a Low Concentration. *ChemSusChem* **2018**, *11*, 2340–2347.
105. Sharma, N.; Dhankhar, S. S.; Kumar, S.; Kumar, D.; Nagaraja, M. Rational Design of a 3D MnII-Metal-Organic Framework Based on a Nonmetallated Porphyrin Linker for Selective Capture of CO_2 and One-Pot Synthesis of Styrene Carbonates. *Chem. Eur. J.* **2018**, *24*, 16662–16669.
106. Ji, J.; Liu, H.; Chen, Z.; Fu, Y.; Yang, W.; Yin, S.-F. Modulating the Acidic and Basic Site Concentration of

DOI: 10.31635/ccschem.024.202403909
Citation: *CCS Chem.* **2024**, 6, 1380–1402
Link to VoR: https://doi.org/10.31635/ccschem.024.202403909

Metal-Organic Framework Derivatives to Promote the Carbon Dioxide Epoxidation Reaction. *Chem. Eur. J.* **2021**, *27*, 11102–11109.
107. Das, R.; Manna, S. S.; Pathak, B.; Nagaraja, C. M. Strategic Design of Mg-Centered Porphyrin Metal-Organic Framework for Efficient Visible Light-Promoted Fixation of CO_2 under Ambient Conditions: Combined Experimental and Theoretical Investigation. *ACS Appl. Mater. Interfaces* **2022**, *14*, 33285–33296.
108. Chen, C.-X.; Rabaâ, H.; Wang, H.; Lan, P. C.; Xiong, Y.-Y.; Wei, Z.-W.; Al-Enizi A. M.; Nafady, A.; Ma, S. In Situ Formation of Frustrated Lewis Pairs in a Zirconium Metal-Organic Cage for Sustainable CO_2 Chemical Fixation. *CCS Chem.* **2023**, *5*, 1989–1998.
109. Navarro-Sánchez, J.; Almora-Barrios, N.; Lerma-Berlanga, B.; Ruiz-Pernía, J. J.; Lorenz-Fonfria, V. A.; Tuñón, I.; Martí-Gastaldo, C. Translocation of Enzymes into a Mesoporous MOF for Enhanced Catalytic Activity under Extreme Conditions. *Chem. Sci.* **2019**, *10*, 4082–4088.
110. Pan, Y.; Li, H.; Lenertz, M.; Han, Y.; Ugrinov, A.; Kilin, D.; Chen, B.; Yang, Z. One-Pot Synthesis of Enzyme@Metal-Organic Material (MOM) Biocomposites for Enzyme Biocatalysis. *Green Chem.* **2021**, *23*, 4466–4476.
111. Leng, F.; Liu, H.; Ding, M.; Lin, Q.-P.; Jiang, H.-L. Boosting Photocatalytic Hydrogen Production of Porphyrinic MOFs: The Metal Location in Metalloporphyrin Matters. *ACS Catal.* **2018**, *8*, 4583–4590.
112. Liao, P.; Hu, Y.; Liang, Z.; Zhang, J.; Yang, H.; He, L.-Q.; Tong, Y.-X.; Liu, J.-M.; Chen, L.; Su, C.-Y. Porphyrin-Based Imine Gels for Enhanced Visible-Light Photocatalytic Hydrogen Production. *J. Mater. Chem. A* **2018**, *6*, 3195–3201.
113. Hu, H.; Zeng, L.; Li, Z.; Zhu, T.; Wang, C. Incorporating Porphyrin-Pt in Light-Harvesting Metal-Organic Frameworks for Enhanced Visible Light-Driven Hydrogen Production. *Chinese J. Catal.* **2021**, *42*, 1345–1351.
114. Liang, Z.; Guo, H.; Lei, H.; Cao, R. Co Porphyrin-Based Metal-Organic Framework for Hydrogen Evolution Reaction and Oxygen Reduction Reaction. *Chinese Chem. Lett.* **2022**, *33*, 3999–4002.
115. Liu, J.; Zhang, K.; Chen, Z.; Wei, Z.-W.; Zhang, L. A Porous and Stable Porphyrin Metal-Organic Framework as an Efficient Catalyst towards Visible-Light-Mediated Aerobic Cross-Dehydrogenative-Coupling Reactions. *Chem. Asian. J.* **2020**, *15*, 1118–1124.
116. Wang, Y.; Zhao, L.; Ji, G.; He, C.; Liu, S.; Duan, C. Vanadium(VIV)-Porphyrin-Based Metal-Organic Frameworks for Synergistic Bimetallic Activation of Inert C(sp^3)-H Bonds. *ACS Appl. Mater. Interfaces* **2022**, *14*, 2794–2804.
117. Sui, J.; Gao, M.-L.; Qian, B.; Liu, C.; Pan, Y.; Meng, Z.; Yuan, D.; Jiang, H.-L. Bioinspired Microenvironment Modulation of Metal-Organic Framework-Based Catalysts for Selective Methane Oxidation. *Sci. Bull.* **2023**, *68*, 1886–1893.
118. Dong, J.; Liu, Y.; Cui, Y. Artificial Metal-Peptide Assemblies: Bioinspired Assembly of Peptides and Metals Through Space and Across Length Scales. *J. Am. Chem. Soc.* **2021**, *143*, 17316–17336.
119. Guo, J.; Duan, Y.; Jia, Y.; Zhao, Z.; Gao, X.; Liu, P.; Li, F.; Chen, H.; Ye, Y.; Liu, Y.; Zhao, M.; Tang, Z.; Liu, Y. Biomimetic Chiral Hydrogen-Bonded Organic-Inorganic Frameworks. *Nat. Commun.* **2024**, *15*, 139.
120. Jiao, L.; Jiang, H.-L. Metal-Organic Frameworks for Catalysis: Fundamentals and Future Prospects. *Chinese J. Catal.* **2023**, *45*, 1–5.
121. Jiao, L.; Yan, H.; Wu, Y.; Gu, W.; Zhu, C.; Du, D.; Lin, Y. When Nanozymes Meet Single-Atom Catalysis. *Angew. Chem. Int. Ed.* **2020**, *59*, 2565–2576.

DOI: 10.31635/ccschem.024.202403909
Citation: *CCS Chem.* **2024**, 6, 1380–1402
Link to VoR: https://doi.org/10.31635/ccschem.024.202403909